

Strong Allee effect synaptic plasticity rule in an unsupervised learning environment

Eddy Kwessi*

Abstract

Synaptic plasticity or the ability of a brain to changes one or more of its functions or structures has generated and is still generating a lot of interest from the scientific community especially neuroscientists. These interests especially went into high gear after empirical evidences were collected that challenged the established paradigm that human brain structures and functions are set from childhood and only modest changes were expected beyond. Early synaptic plasticity rules or laws to that regard include the basic Hebbian rule that proposed a mechanism for strengthening or weakening of synapses (weights) during learning and memory. This rule however did not account from the fact that weights must have bounded growth overtime. Thereafter, many other rules were proposed to complement the basic Hebbian rule and they also posses other desirable properties. In particular, a desirable property in synaptic plasticity rule is that the ambient system must account for inhibition which is often achieved if the rule used allows for a lower bound in synaptic weights. In this paper, we propose a synaptic plasticity rule inspired from the Allee effect, a phenomenon often observed in population dynamics. We show properties such such as synaptic normalization, competition between weights, de-correlation potential, and dynamic stability are satisfied. We show that in fact, an Allee effect in synaptic plasticity can be construed as an absence of plasticity.

1 Introduction

Synapses play an important role in the brain because they are junctions between nerves cells. As such, they facilitate diffusion of chemical substances called neurotransmitters from the brain to other parts of the body. During this diffusion, synapses are sometimes modified to adapt to the impulses and their transmission rate. These synaptic modifications may be due to lived experience and training and can occur at functional and structural levels. At a functional level, the brain may move functions from one area to other areas, often between damaged to undamaged ones. At a structural level, the brain may actually change its physical structure, mainly some synaptic structures as a result of external activities. Synapses modifications can in turn affect behavior and training, therefore, understanding the dichotomy between synaptic modifications and

*Corresponding author: Department of Mathematics, Trinity University, 1 Trinity Place, San Antonio, TX 78212, Email: ekwessi@trinity.edu

experience and/or training is paramount if one wants to have an insight into some of our brain activities. Brain plasticity or neuroplasticity can be thought of as the ability of the brain to adapt to external activities by reorganizing some of its pathways or by modifying some of its synaptic structure. Changes in the brain were believed to occur only during infancy and early childhood so that the brain structure was believed to be mostly set by adulthood. Pioneers challenging this paradigm include [James \(1890\)](#), who suggested that in fact, at any age, the brain, just like any organic matter, has a great deal of plasticity. Early researchers on synaptic plasticity include [Hebb \(1949\)](#), who conjectured that on one hand, synapses from two neurons are often strengthened if impulses from one neuron contribute to the firing of another. On the other hand, synapses are weakened if non-coincidental neuronal firings occur. In essence, this rule infers that synaptic modifications are in direct relationship with experience and training, and consequently, the mechanisms underlying learning and memory can be understood via these synaptic modifications. In fact, there is ample empirical evidence consisting of transient and long lasting effects (long-term potentiation and depression) starting with [Bliss and Lomo \(1973\)](#) who experimented plasticity in rabbits. Plasticity was later experimented in selected regions of the brains like the hippocampus neocortex and cerebellum, see for instance [Bear and Malenka \(1994\)](#); [Bliss and Lomo \(1973\)](#); [Bussey \(2011\)](#); [Feldman \(2009\)](#); [Liu and Nusslock \(2018a,b\)](#); [Olson et al. \(2006\)](#); [Siegelbaum and Kandel \(1991\)](#); [Xu and Kang \(2005\)](#). Learning and memory are therefore manifestations of the brain's capacity to sustain recurrent changes. Moreover, it has been documented that the main excitatory neurotransmitter in the mammalian nervous system is L-glutamate, see [Voglis and Tavernarakis \(2006\)](#). This transmitter is usually detected at postsynaptic terminals by a coupling of G-protein and inotropic glutamate receptors who have been associated with learning and memory, see [Bliss and Collingridge \(1997\)](#). Plasticity also plays a role in various pathologies. For instance, following a stroke, evidence has emerged linking pathological neural plasticity or postischemic long-term potentiation with ischemia which is a deficiency of blood to the heart or to the brain, see [Wang et al. \(2014\)](#). Pathological neural plasticity also plays an important role in epilepsy, another pathology that is said to arise from malfunction of a mutated ion channel, leading to increased excitatory or decreased inhibitory currents, see [Swann and Nishimura \(2009\)](#); [Wimmer et al. \(2009\)](#). Other neurological disorders have been linked with plasticity, for instance Alzheimer's disease, Parkinson's disease, Huntington's disease, dystonia, see [Dorszewska et al. \(2020\)](#); [Thickbroom and Mastaglia \(2009\)](#). However, to understand plasticity at the functional level, one needs to go beyond mechanistic models as described above and find how plasticity relates neurons and/or network of neurons to the basic rules that govern its induction, see [Dayan and Abbott \(2001\)](#). This entails finding mechanisms relating the strengthening or weakening of synapses via neurotransmitters and (presynaptic) neurons. Many mathematical models or synaptic plasticity rules have been proposed to explain synaptic plasticity in supervised and unsupervised learning environments. In an unsupervised learning environment where the neurons network self-organizes, an activity is represented by a continuous variable (input) at the presynaptic level and linked to a postsynaptic activity variable (output) by dynamic weights. The relationship between these variables is a differential equation describing the change of weights overtime and include and is not limited to the Basic Hebbian rule ([Sejnowski and Tesauro \(1989\)](#)) and its variant the Covariance rule ([Dayan and Abbott \(2001\)](#)), the Bienestock-Cooper-Munro (BCM)

rule (Bienenstock et al. (1982)), and the Oja rule (Oja (1982)). To avoid unbounded growth, an upper saturation limit is often imposed, for instance in BCM and Oja rules. A lower limit is needed to allow for inhibition. However, this lower limit is often given by the condition that the length of weights not be zero. In populations dynamics, there are rules for which the density or size of a population is both bounded above and below by nonnegative constants as in the Allee effect. The Allee effect was introduced by Allee (1949) and characterizes a phenomenon in population dynamics where there is a positive correlation between a population density or size and its per capita growth rate. In the literature, Allee effects are divided into strong and weak Allee effects, see for instance Hutchings (2015). The strong Allee effect occurs when a population has a critical density A below which it declines to extinction while the weak Allee effect occurs when a population lacks such a critical density, but at lower densities, the population growth rate arises with increasing densities. Since their inception, Allee effects have substantially been investigated and applied by researchers across the board. Ecology is probably the area where researchers have investigated it the most. Mathematical models of the Allee effects and their dynamics have been investigated for competing populations in Assas et al. (2014, 2015a,b,c); Elaydi et al. (2018). Stochastic models of the Allee effects were discussed in Assas et al. (2016). Models addressing Allee effects and conservation are discussed in Courchamp et al. (2008). Models addressing population resilience were proposed by Dennis et al. (2015). Some real life evidence of Allee effects have been documented in Courchamp et al. (2008); Perala and Kuparinen (2017). Possible extension of Allee effects to medicine have been proposed in Delitala et al. (2020); Fontanari and Perlovsky (2006); Johnson et al. (2019); Konstorum et al. (2016); Neufeld et al. (2017). It has been speculated that the passenger pigeon, who was once the most abundant bird in North America and now extinct, was subject to a phenomenon similar to an Allee effect, see for instance Avery (2014); Fuller (2014); Greensberg (2014). The endangered Vancouver Island marmots, who are on the brink of extinction, may be subject to an Allee effect as well, see for instance Brashares et al. (2010).

Figure 1 below is an illustration of the different types of Allee effects, where A is the critical (Allee) density and K is the carrying capacity of the population.

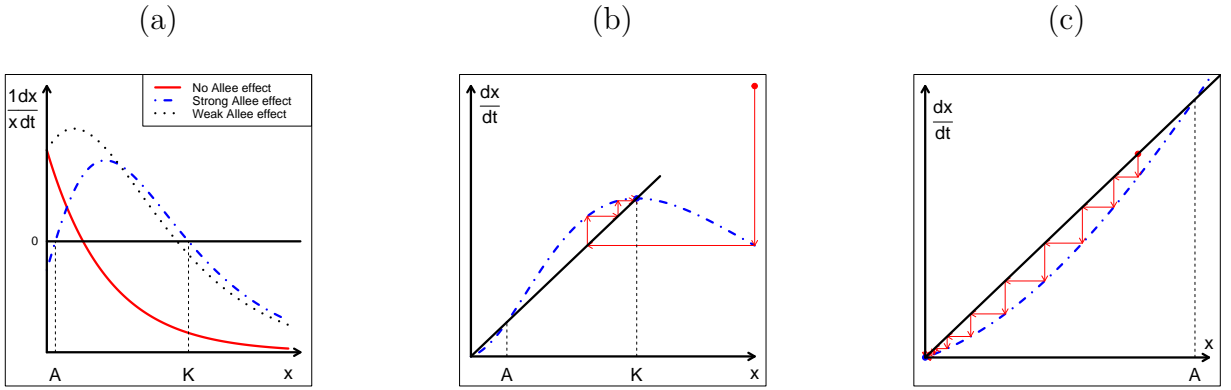


Figure 1: In (a), represented is the per capita growth rate as a function of the population density x . The red curve represents no Allee effect, the black dashed curve represents the weak Allee effect, blue dashed represents the strong Allee effect. In (b), the strong Allee effect is represented. A starting trajectory (red arrows) above A converge to K . In (c), by zooming closer A , we observe that a starting trajectory below A converges to 0.

To our knowledge, the Allee effect has not yet been discussed in combination with plasticity rules. In this paper, we aim to make a foray on the topic and we show that in fact, an Allee effect, when combined to the Oja rule, can be characterized as a drift toward an absence of plasticity. Moreover, the model we propose has the following key advantages.

1. Unbounded growth is controlled.
2. Multiplicative normalization is preserved.
3. Competition between weights is induced.
4. The model is general enough to account for multiple layers of pre-and postsynaptic neurons.
5. Under specific conditions on the network parameters, stability of dynamical system is obtained.

The use of an Allee effect in neuroscience may have the potential to produce invaluable information that could highlight hidden features in plasticity and could potentially enrich the ever growing literature on the topic. The remainder of this paper is organized as follows: In Section 2, we introduce our idea of the an Allee effect postsynaptic neuron model. In Section 3, we discuss stability analysis of s single postsynaptic neuron model, with and without a plastic recurrent connection. Ensembles of postsynaptic neurons are tackled in Section 4.

2 Allee effect postsynaptic neuron model and motivation

Consider a system with L layers and let a $L \times N_u$ matrix $\mathbf{u} = (\mathbf{u}^{(1)}, \mathbf{u}^{(2)}, \dots, \mathbf{u}^{(L)})$ represent the presynaptic activities in the system. For $1 \leq \ell \leq L$, $\mathbf{u}^{(\ell)} = (u_1^{(\ell)}, u_2^{(\ell)}, \dots, u_{N_u}^{(\ell)})$ represents presynaptic activities of N_u inputs or neurons within the ℓ th layer of the system. Let a $L \times N_v$ matrix $\mathbf{v} = (\mathbf{v}^{(1)}, \mathbf{v}^{(2)}, \dots, \mathbf{v}^{(L)})$ be the postsynaptic activities generated by the presynaptic activities \mathbf{u} , where $\mathbf{v}^{(\ell)} = (v_1^{(\ell)}, v_2^{(\ell)}, \dots, v_{N_v}^{(\ell)})$ represents the postsynaptic activities of N_v neurons on the ℓ th layer. Let \mathbf{W} be an input synaptic block-matrix of weights representing the strengths of the synapses from the presynaptic neurons \mathbf{u} to the postsynaptic neurons \mathbf{v} . We note that \mathbf{W} is an $L \times N_u \times L \times N_v$ block-matrix with entries $(\mathbf{W}^{(k,\ell)})$, for $1 \leq k, \ell \leq L$. Each block $\mathbf{W}^{(k,\ell)}$ is a matrix with entries $w_{ij}^{(k,\ell)}$ where $1 \leq j \leq N_v$ and $1 \leq i \leq N_u$. To account for inter-connections between postsynaptic neurons, we will consider an $L \times N_v \times L \times N_v$ recurrence block-matrix \mathbf{Z} with entries $\mathbf{Z}^{(k,\ell)}$, for $1 \leq k, \ell \leq L$, where each entry $\mathbf{Z}^{(k,\ell)}$ is a matrix with entries $z_{mj}^{(k,\ell)}$ for $1 \leq j, m \leq N_v$. We let $d_w = L \times N_u \times L \times N_v$ and $d_z = L \times N_v \times L \times N_v$ and we define the length of a vector \mathbf{W} in \mathbb{R}^{d_w} as $\|\mathbf{W}\|^2 = \mathbf{W}^T \cdot \mathbf{W}$, where the dot stands for the dot or inner product in \mathbb{R}^{d_w} .

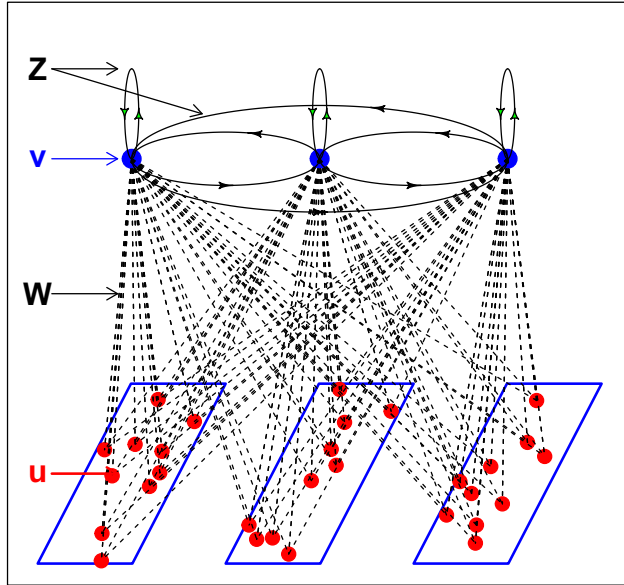


Figure 2: A geometric representation of a triple-layer architecture with $N_u = 10$ presynaptic neurons $u_j^{(\ell)}$ and $N_v = 1$ postsynaptic neurons $v_i^{(\ell)}$ per layer, $d_w = 90$ weights $w_{ik}^{(k,\ell)}$, and $d_z = 9$ recurrent connections $z_{im}^{(k,\ell)}$.

Remark 1. *In the sequel, we will use invariably the dot product with the following understanding:*

$\mathbf{W}^T \cdot \mathbf{u}$ is an $L \times N_v$ matrix with entries

$$(\mathbf{W}^T \cdot \mathbf{u})_i^{(k)} = \sum_{\ell=1}^L \sum_{j=1}^{N_u} w_{ij}^{(k,\ell)} u_j^{(\ell)}, \quad \text{for } 1 \leq k \leq L, 1 \leq i \leq N_v.$$

$\mathbf{Z}^T \cdot \mathbf{v}$ is an $L \times N_v$ matrix with entries

$$(\mathbf{Z}^T \cdot \mathbf{v})_i^{(k)} = \sum_{\ell=1}^L \sum_{m=1}^{N_v} z_{im}^{(k,\ell)} v_m^{(\ell)} \quad \text{for } 1 \leq k \leq L, 1 \leq i \leq N_v.$$

Consequently, as sums of products of coordinates of vectors, entries for $\mathbf{W}^T \cdot \mathbf{u}$ and $\mathbf{Z}^T \cdot \mathbf{v}$ are themselves dot products and therefore enjoy their properties. Also in the sequel, matrices and vectors and will be represented by bold face symbols whereas scalars will be represented by normal font symbols.

Definition 2. The learning activity of a system or plasticity function of a system is a function given as

$$L(\mathbf{W}, \mathbf{u}, \mathbf{v}) = H(\mathbf{W}, \mathbf{u}, \mathbf{v}) - \varphi(\mathbf{W}, \mathbf{u}, \mathbf{v}), \quad (2.1)$$

where $H(\mathbf{W}, \mathbf{u}, \mathbf{v})$ is a function referred to as the Hebbian function and $\varphi(\mathbf{W}, \mathbf{u}, \mathbf{v})$ is function referred to as the Hebbian modification function.

Definition 3. We define a synaptic plasticity rule as

$$\tau_{\mathbf{w}} \frac{d\mathbf{W}}{dt} = L(\mathbf{W}, \mathbf{u}, \mathbf{v}). \quad (2.2)$$

The constant $\tau_{\mathbf{w}}$ represents a time scaling constant controlling the rate of change of \mathbf{W} and $\lambda_{\mathbf{w}} = \frac{1}{\tau_{\mathbf{w}}}$ represents the learning rate. The model in equation (2.2) is general enough to include many known synaptic plasticity rules. For instance,

- If $H(\mathbf{W}, \mathbf{u}, \mathbf{v}) = \mathbf{v}^T \mathbf{u}$ and $\varphi(\mathbf{W}, \mathbf{u}, \mathbf{v}) = 0$, we obtain the Basic Hebb rule, see [Hebb \(1949\)](#).
- If $H(\mathbf{W}, \mathbf{u}, \mathbf{v}) = \mathbf{v}^T \mathbf{u}$ and $\varphi(\mathbf{W}, \mathbf{u}, \mathbf{v}) = \theta_{\mathbf{v}} \mathbf{u}$ or $\varphi(\mathbf{W}, \mathbf{u}, \mathbf{v}) = \theta_{\mathbf{u}} \mathbf{v}^T$ for some constants $\theta_{\mathbf{u}}$ and $\theta_{\mathbf{v}}$, we obtain the Covariance rule, see [Dayan and Abbott \(2001\)](#).
- If $H(\mathbf{W}, \mathbf{u}, \mathbf{v}) = \mathbf{v} \mathbf{v}^T \mathbf{u}$ and $\varphi(\mathbf{W}, \mathbf{u}, \mathbf{v}) = \theta_{\mathbf{v}} \mathbf{v}^T \mathbf{u}$, for some constant $\theta_{\mathbf{v}}$, we obtain the Bienenstock-Cooper-Munro (BCM) rule, see [Bienenstock et al. \(1982\)](#).
- If $H(\mathbf{W}, \mathbf{u}, \mathbf{v}) = \mathbf{v}^T \mathbf{u}$ and $\varphi(\mathbf{W}, \mathbf{u}, \mathbf{v}) = \alpha \mathbf{v}^T \mathbf{W} \mathbf{v}$, for some positive constant α , then we obtain the Oja rule, see [Oja \(1982\)](#).

To model the dynamics of postsynaptic neurons \mathbf{v} , we will use the firing-rate equation given as

$$\tau_{\mathbf{v}} \frac{d\mathbf{v}}{dt} = -\mathbf{v} + T(\mathbf{W}, \mathbf{Z}, \mathbf{u}, \mathbf{v}), \quad (2.3)$$

where $\tau_{\mathbf{v}}$ represents the time scale of the firing-rate dynamics of \mathbf{v} and $T(\mathbf{W}, \mathbf{Z}, \mathbf{u}, \mathbf{v})$ is a function representing the total activity in the system. This activity may consist of pre- and postsynaptic activities \mathbf{u} and \mathbf{v} , with feed-forward and/or feed-backward connections

with intensities (or weights) \mathbf{W} , with or without recurrent connections with intensities \mathbf{Z} . In the general literature, $T(\mathbf{W}, \mathbf{Z}, \mathbf{u}, \mathbf{v})$ is taken as a linear function of the pre-and postsynaptic activities \mathbf{u} and \mathbf{v} . That is, $T(\mathbf{W}, \mathbf{Z}, \mathbf{u}, \mathbf{v}) = \mathbf{W}^T \cdot \mathbf{u} + \mathbf{Z}^T \cdot \mathbf{v}$. It can also be a nonlinear function depending on an activation function G as $T(\mathbf{W}, \mathbf{Z}, \mathbf{u}, \mathbf{v}) = G(\mathbf{W}^T \cdot \mathbf{u} + \mathbf{Z}^T \cdot \mathbf{v})$ or two activation functions G_1 and G_2 as $T(\mathbf{W}, \mathbf{Z}, \mathbf{u}, \mathbf{v}) = \mathbf{W}^T \cdot G_1(\mathbf{u}) + \mathbf{Z}^T \cdot G_2(\mathbf{v})$. The activation function controls the rate of signals emitted by presynaptic neurons \mathbf{u} and the recurrence rate of postsynaptic neurons \mathbf{v} . It is common to use either the sigmoid function $G(x) = (1 + e^{-x})^{-1}$ or the Heaviside function $G(x) = 0, x < 0, G(x) = 1, x > 0$. We observe however that more general activation functions G can be considered, see for instance Kwessi (2021a). We note that a more complete and perhaps more realistic model for equation (2.3) should contain a diffusion term and a less trivial reaction term than \mathbf{v} . For sake of simplicity and to maintain tractability, we will not do so in the present discussion.

Remark 4. *It is important to note that here, the total activity, $T(\mathbf{W}, \mathbf{Z}, \mathbf{u}, \mathbf{v})$ would be zero if the pre-and and postsynaptic activities \mathbf{u} and \mathbf{v} are canceling each other. This is obviously the case if $\mathbf{u} = 0$ and $\mathbf{v} = 0$. From equation (2.3) above, if $T(\mathbf{W}, \mathbf{Z}, \mathbf{u}, \mathbf{v}) = 0$, then $\mathbf{v}(t) = \mathbf{v}_0 e^{-\lambda_v t}$ and thus approaches 0 overtime. Combining the latter with (2.2), it follows, for some constant presynaptic inputs \mathbf{u} and for some generic constant matrix Σ that*

- $\mathbf{W}(t) = \frac{\lambda_w}{\lambda_v} [e^{-\lambda_v t} \mathbf{v}_0^T \mathbf{u} + \Sigma]$ for the Basic Hebb rule.
- $\mathbf{W}(t) = \frac{\lambda_w}{\lambda_v} [e^{-\lambda_v t} \mathbf{v}_0^T (\mathbf{u} - \theta_v) + \Sigma]$ or $\mathbf{W}(t) = \frac{\lambda_w}{\lambda_v} [e^{-\lambda_v t} \mathbf{v}_0^T (\theta_u - \mathbf{u}) + \Sigma]$ for the Covariance rule.
- $\mathbf{W}(t) = \frac{\lambda_w}{\lambda_v} \left[\left(\frac{e^{-\lambda_v t}}{2} \mathbf{v}_0^T - \theta_v \right) e^{-\lambda_v t} \mathbf{v}_0^T \mathbf{u} + \Sigma \right]$ for the BCM rule.
- $\mathbf{W}(t) = e^{\mathbf{v}_0^T \mathbf{v}_0 \frac{\alpha}{2\lambda_v} e^{-2\lambda_v t}} \left[\mathbf{v}_0^T \mathbf{u} \int e^{-\lambda_v t - \mathbf{v}_0^T \mathbf{v}_0 \frac{\alpha}{2\lambda_v} e^{-2\lambda_v t}} dt + \Sigma \right]$ for the Oja rule.

We can therefore infer that when $T(\mathbf{W}, \mathbf{Z}, \mathbf{u}, \mathbf{v}) = 0$, \mathbf{v} approaches 0 overtime whereas \mathbf{W} approaches a constant Σ . Moreover, if $T(\mathbf{W}, \mathbf{Z}, \mathbf{u}, \mathbf{v}) = \mathbf{W}^T \cdot \mathbf{u} + \mathbf{Z}^T \cdot \mathbf{v} = 0$, the constant Σ must be zero or the presynaptic activities \mathbf{u} must be zero.

Remark 5. *We also observe that $T(\mathbf{W}, \mathbf{Z}, \mathbf{u}, \mathbf{v}) = \mathbf{W}^T \cdot \mathbf{u} + \mathbf{Z}^T \cdot \mathbf{v}$ can be understood as the total potential energy in the system. Indeed, suppose $\mathbf{W}, \mathbf{Z}, \mathbf{u}$, and \mathbf{v} are vector fields over an open connected domain \mathcal{D} . Let P be a path in \mathcal{D} . If these fields are continuous over \mathcal{D} and $\int_P \mathbf{W}^T \cdot d\mathbf{u}$ and $\int_P \mathbf{u} \cdot d\mathbf{W}^T$ are path-independent, then the fields \mathbf{W} and \mathbf{u} are conservative. Consequently, there exist functions f_1 and f_2 such that $\mathbf{W}^T = \nabla f_1$ and $\mathbf{u} = \nabla f_2$. Therefore, the potential energy due to the fields \mathbf{W}^T and \mathbf{u} is*

$$\int_P \nabla f_1 \cdot d\mathbf{u} + \int_P \nabla f_2 \cdot d\mathbf{W} = \mathbf{W}^T \cdot \mathbf{u}.$$

Similarly, there exist functions g_1 and g_2 such that the potential energy due to the fields \mathbf{Z} and \mathbf{v} is

$$\int_P \nabla g_1 \cdot d\mathbf{v} + \int_P \nabla g_2 \cdot d\mathbf{Z}^T = \mathbf{Z}^T \cdot \mathbf{v}.$$

From equation (2.3), we can deduce that the steady state is attained when the postsynaptic activity is equal to the total potential energy in the system. This also suggests that postsynaptic activity increases if it is less than the system's potential energy and decreases otherwise.

In this paper, we will make the following considerations : for nonnegative constants A, K , in equation (2.2), we put

$$\begin{aligned} H(\mathbf{W}, \mathbf{u}, \mathbf{v}) &= [\mathbf{1} - A(\mathbf{W}^T \mathbf{W})^{-1}] \mathbf{v}^T \mathbf{u} \\ \varphi(\mathbf{W}, \mathbf{u}, \mathbf{v}) &= K^{-1} [\mathbf{1} - A(\mathbf{W}^T \mathbf{W})^{-1}] \mathbf{v}^T \mathbf{W} \mathbf{v}, \end{aligned}$$

where $\mathbf{1}$ is a matrix with entries ones and with the same dimension as the matrix $(\mathbf{W}^T \mathbf{W})^{-1}$. Equation (2.2) can now be written as

$$\tau_{\mathbf{w}} \frac{d\mathbf{W}}{dt} = \mathbf{v}^T (\mathbf{u} - K^{-1} \mathbf{W} \mathbf{v}) (\mathbf{1} - A(\mathbf{W}^T \mathbf{W})^{-1}) . \quad (2.4)$$

Let us now give a motivation for the model in equation (2.4). Suppose that we have only one layer ($L = 1$) and a single postsynaptic neuron ($N_v = 1$). Therefore $\mathbf{v} = v$ will be a scalar. Let us assume further that there is no recurrent connection ($\mathbf{Z} = \mathbf{0}$). Per Remark 1, $\mathbf{W}^T \cdot \mathbf{u}$ will be a scalar. Moreover, \mathbf{W} is a $1 \times N_u$ vector, thus $\mathbf{W}^T \cdot \mathbf{W} = \|\mathbf{W}\|^2$ is a positive scalar. Equation (2.4) becomes

$$\tau_{\mathbf{w}} \frac{d\mathbf{W}}{dt} = v (\mathbf{u} - K^{-1} v \mathbf{W}) (\mathbf{1} - A(\|\mathbf{W}\|^2)^{-1}) . \quad (2.5)$$

Thus, if we take the dot product on both sides of equation (2.4) by \mathbf{W}^T and multiply by the constant 2, it becomes

$$2\tau_{\mathbf{w}} \mathbf{W}^T \cdot \frac{d\mathbf{W}}{dt} = \tau_{\mathbf{w}} \frac{d\|\mathbf{W}\|^2}{dt} = 2v \left(\mathbf{W}^T \cdot \mathbf{u} - \frac{v}{K} \|\mathbf{W}\|^2 \right) \left(1 - \frac{A}{\|\mathbf{W}\|^2} \right) . \quad (2.6)$$

Consequently, the system composed of equations (2.6) and (2.3) arrives at its steady states, given by the equation of its v -isocline $\left(\frac{dv}{dt} = 0 \right) v = T(\mathbf{W}, \mathbf{u}, v)$ and the equations of its $\|\mathbf{W}\|^2$ -isocline $\left(\frac{d\|\mathbf{W}\|^2}{dt} = 0 \right)$ given as $v = 0$, $\|\mathbf{W}\|^2 = A$, and $\mathbf{W}^T \cdot \mathbf{u} - \frac{v}{K} \|\mathbf{W}\|^2 = 0$. In the linear case in particular, we have $v = T(\mathbf{W}, \mathbf{u}, v) = \mathbf{W}^T \cdot \mathbf{u}$. Therefore, we obtain that either $\|\mathbf{W}\|^2 = A$ or $\|\mathbf{W}\|^2 = K$ when the steady states are reached. Similarly to a strong Allee effect, the lengths of weights $\|\mathbf{W}\|^2$ below $\min\{A, K\}$ will decay to zero overtime, which means that postsynaptic activities will decrease towards a state of no activity at all. We note also that when $A = 0$, equation (2.4) becomes the Oja rule. In population dynamics in general, the term $(1 - A \|\mathbf{W}\|^{-2})$ is used to account for the presence of sparse populations or mate limitation. Adding this term as in equation (2.6) induces the synaptic normalization in that when the weights are nonnegative, their growth is limited by the global thresholds A or K , see Figure 5–9 below, in the case of a single neuron. Moreover, convergence of $\|\mathbf{W}\|^2$ toward K induces competition between weights and preserves dynamic stability. In conclusion, the model in equation (2.4) is a matrix equivalent of equation (2.5) when we account for multiple layers and multiple postsynaptic neurons. In light of these facts, we will combine equation (2.4) and (2.3) for the definition of an Allee plasticity rule.

Definition 6. An Allee effect is a synaptic plasticity rule having a treshhold under which, activities drift towards an absence of plasticity and above which activities eventually become stable.

Definition 7. Let $\mathbf{W}, \mathbf{Z}, \mathbf{u}$, and \mathbf{v} be given as above. Consider an activity function $T(\mathbf{W}, \mathbf{Z}, \mathbf{u}, \mathbf{v})$. We define an Allee plasticity rule with non plastic recurrent connections as the system of differential equations

$$\begin{cases} \tau_{\mathbf{w}} \frac{d\mathbf{W}}{dt} &= \mathbf{v}^T (\mathbf{u} - K^{-1}\mathbf{W}\mathbf{v}) (\mathbf{1} - A(\mathbf{W}^T\mathbf{W})^{-1}) \\ \tau_{\mathbf{v}} \frac{d\mathbf{v}}{dt} &= -\mathbf{v} + T(\mathbf{W}, \mathbf{Z}, \mathbf{u}, \mathbf{v}) \end{cases} . \quad (2.7)$$

Definition 8. We define an Allee plasticity rule with plastic recurrent connections as the system of differential equations

$$\begin{cases} \tau_{\mathbf{w}} \frac{d\mathbf{W}}{dt} &= \mathbf{v}^T (\mathbf{u} - K^{-1}\mathbf{W}\mathbf{v}) (\mathbf{1} - A(\mathbf{W}^T\mathbf{W})^{-1}) \\ \tau_{\mathbf{v}} \frac{d\mathbf{v}}{dt} &= -\mathbf{v} + T(\mathbf{W}, \mathbf{Z}, \mathbf{u}, \mathbf{v}) \\ \tau_{\mathbf{z}} \frac{d\mathbf{Z}}{dt} &= R(\mathbf{W}, \mathbf{Z}, \mathbf{u}, \mathbf{v}) \end{cases} . \quad (2.8)$$

where $R(\mathbf{W}, \mathbf{Z}, \mathbf{u}, \mathbf{v})$ is the total *recurrent (post-synaptic) activity* and $\tau_{\mathbf{z}}$ is a scaling constant. In the literature, two rules are often considered for $R(\mathbf{W}, \mathbf{Z}, \mathbf{u}, \mathbf{v})$, see for instance see [Dayan and Abbott \(2001\)](#).

- Anti-Hebbian rule: $R(\mathbf{W}, \mathbf{Z}, \mathbf{u}, \mathbf{v}) = -\mathbf{v}^T\mathbf{v} + \beta\mathbf{Z}$, for some constant β .
- Goodall rule: $R(\mathbf{W}, \mathbf{Z}, \mathbf{u}, \mathbf{v}) = \mathbf{I} - (\mathbf{W}^T \cdot \mathbf{u})\mathbf{v} - \mathbf{Z}$. This rule is often used because it produces de-corrallated postsynaptic outputs and possess homoschedasticity properties.

In the next sections, we will discuss stability analysis of these plasticity rules.

3 Stability analysis of a single postsynaptic neuron model

Here, we let $L = 1$ and $N_v = 1$. In the presence of a single postsynaptic neuron, the matrix \mathbf{v} is reduced to a constant v and the recurrent connection matrix \mathbf{Z} is reduced to a single constant z . There are two cases to consider: firstly, there could be no recurrent connection between v and itself ($z = 0$), see Figure 3 (a) below. Secondly, there could be a recurrent connection with weight $z \neq 0$, see Figure 3 (b) below.

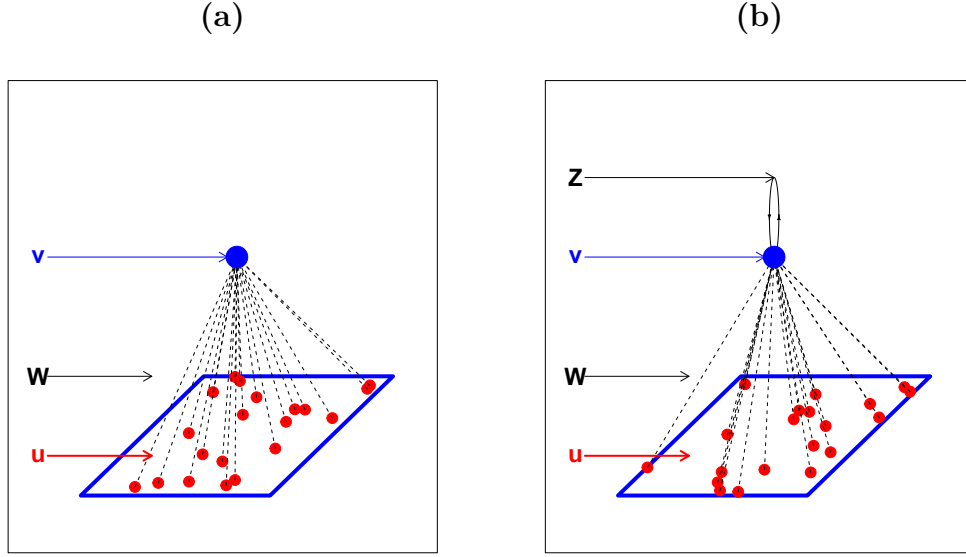


Figure 3: In (a), we have one postsynaptic neuron with no recurrent connection. In (b), we have one postsynaptic neuron with one recurrent connection.

3.1 Single postsynaptic neuron with no recurrent connection

In this case, we will have $\mathbf{Z} = 0$ and $\mathbf{v} = v$. For sake of simplification, we let $T(\mathbf{W}, 0, \mathbf{u}, v) = T(\mathbf{W}, \mathbf{u})$. As we observe above, we consider the scalar auxiliary Allee-type system given by

$$\begin{cases} \tau_{\mathbf{w}} \frac{d\|\mathbf{W}\|^2}{dt} &= 2v \left(\mathbf{W}^T \cdot \mathbf{u} - \frac{v}{K} \|\mathbf{W}\|^2 \right) \left(1 - \frac{A}{\|\mathbf{W}\|^2} \right) \\ \tau_v \frac{dv}{dt} &= -v + T(\mathbf{W}, \mathbf{u}) \end{cases} \quad (3.1)$$

Remark 9. *The steady states of this system will be given by the v -isocline $v = T(\mathbf{W}, \mathbf{u})$ and the $\|\mathbf{W}\|^2$ -isocline $v = 0$, $\|\mathbf{W}\|^2 = A$, or $\frac{\mathbf{W}^T \cdot \mathbf{u}}{\|\mathbf{W}\|^2} = \frac{1}{K} T(\mathbf{W}, \mathbf{u})$. The latter equation has a geometric interpretation. Indeed, this means that within the sphere with radius $r = \|\mathbf{W}\|$, $\frac{1}{K} T(\mathbf{W}, \mathbf{u})$ is the scalar projection of \mathbf{u} onto the vector \mathbf{W} whereas $\frac{1}{K} T(\mathbf{W}, \mathbf{u}) \mathbf{W}$ is the vector projection of \mathbf{u} onto the vector \mathbf{W} , see Figure 4 below.*

We will use the notation $x =: \|\mathbf{W}\|^2$, $y := v$, $u = \|\mathbf{u}\| \cos(\theta)$, where θ is the angle between the vector \mathbf{W} and \mathbf{u} . Thus for suitable functions $f_1(x, u)$ and $f_2(x, u)$, this system is of the form

$$\begin{cases} \tau_x \frac{dx}{dt} &= g_1(x, y) := 2y \left(f_1(x, u) - \frac{yx}{K} \right) \left(1 - \frac{A}{x} \right) \\ \tau_y \frac{dy}{dt} &= g_2(x, y) := -y + f_2(x, u) \end{cases} \quad (3.2)$$

Let us discuss the local stability of the steady state $(A, f_2(A, u))$.

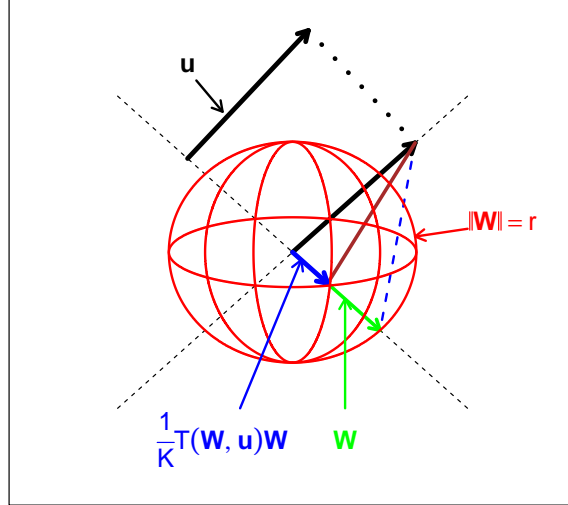


Figure 4: Geometric interpretation of $\frac{1}{K}T(\mathbf{W}, \mathbf{u})\mathbf{W}$ when the steady state is attained.

Theorem 10. Consider the system (3.2). Put $a_0 = f_1(A, u)$ and $b_0 = f_2(A, y, u)$, $c_0 := \frac{\partial f_2(A, u)}{\partial x}$.

- (i) The line $y = 0$ for all $x > 0$ is always a spiral sink.
- (ii) If $b_0(a_0K - b_0A) < 0$, then the steady state (A, b_0) is asymptotically stable.
- (iii) If $b_0(a_0K - b_0A) > 0$, then (A, b_0) is unstable (repeller).
- (iv) If $(a_0K - b_0A) = 0$, the steady state (A, b_0) is a saddle.

Remark 11. (a) We note that the classification of a steady state is independent of the sign of u because $\Delta, \text{tr}(J)$, and $\det(J)$ all depend on u^2 .

- (b) We also note that dynamics of the system in the nonlinear case where $T_2(\mathbf{W}, \mathbf{u}, v) = \mathbf{W} \cdot G(\mathbf{u})$ for some nonlinear function G are similar to that of the linear case. Special care needs to be taken in the case of the steady state $(x, 0)$. This would require, per remark 4 above, that $G(\mathbf{u}) = \mathbf{0}$. Since $G(x) > 0$ for all $x \in \mathbb{R}$, $(x, 0)$ cannot be a steady state. In the case of the Heaviside activation function, $(x, 0)$ is a steady state only when the presynaptic activities are negative (in inhibition), otherwise, it is not a steady state.

In Figure 5–9 below, we will illustrate the above results by plotting the time series of x_t and y_t , for $t = 0, \dots, 250$. We let A and K take interchangeably the values 1.5 and 3 in Figure 5, 6, 8. The starting points of the trajectories are $(0.1, -2)$, $(0.2, -0.9)$ in black color, $(0.3, 1.1)$, $(0.4, 1.5)$ in cyan color, $(4.8, 1)$, $(5, 2)$ in brown color, and $(9.8, -2)$, $(4.5, -2)$ in magenta color. In Figure 5, 6, 7, 9, we take $u = 0.3$. The solid blue curve represents

the x -isocline $f_1(x, u) - \frac{yx}{K} = 0$ which, in the linear case, is given as $y = \frac{uK}{\sqrt{x}}$. The solid blue line represents the x -isocline $y = 0$ and the solid red curve represents the y -isocline $y = f_2(x, u)$ which, in the linear case, is given as $y = u\sqrt{x}$. The dots are the intersection between the x - and y -isoclines. In particular, the gray dot represents the origin $(0, 0)$, the yellow dot has coordinates $(A, u\sqrt{A})$, and is the intersection between the x -isocline $x = A$ and the y -isocline $y = u\sqrt{x}$. Likewise, the green dot is the intersection between the x -isocline $x = K$ and the y -isocline $y = u\sqrt{x}$ with coordinates $(K, u\sqrt{K})$. From these figures, we confirm the results above in that $(A, u\sqrt{A})$ and $(K, u\sqrt{K})$ are either attractors or saddle points. Figure 8 confirms that when $u = 0$, the line $y = 0$ is a sink.

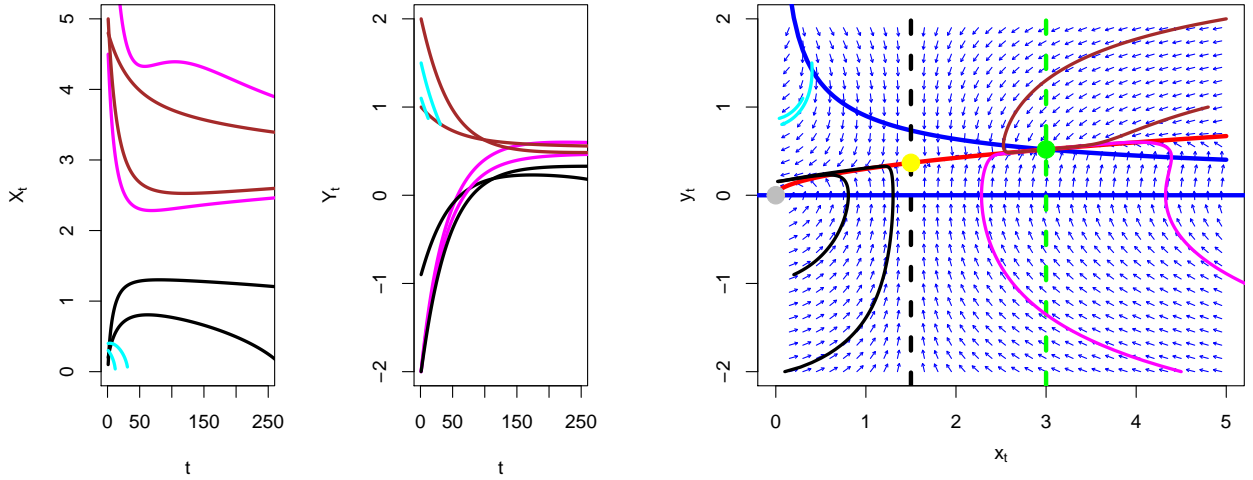


Figure 5: Time series and phase space diagram when $A = 1.5$ and $K = 3$. The point $(A, u\sqrt{A})$ is repeller and $(K, u\sqrt{K})$ is an attractor.

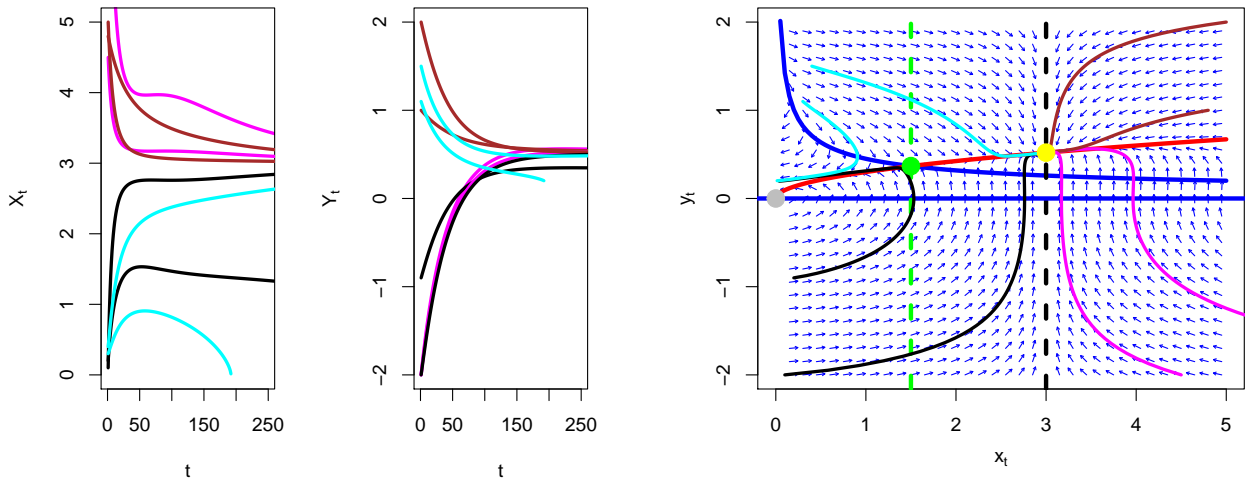


Figure 6: Time series and phase space diagram when $A = 3$ and $K = 1.5$. The point $(A, u\sqrt{A})$ is an asymptotically stable (attractor) and $(K, u\sqrt{K})$ is neither an attractor nor a repeller.

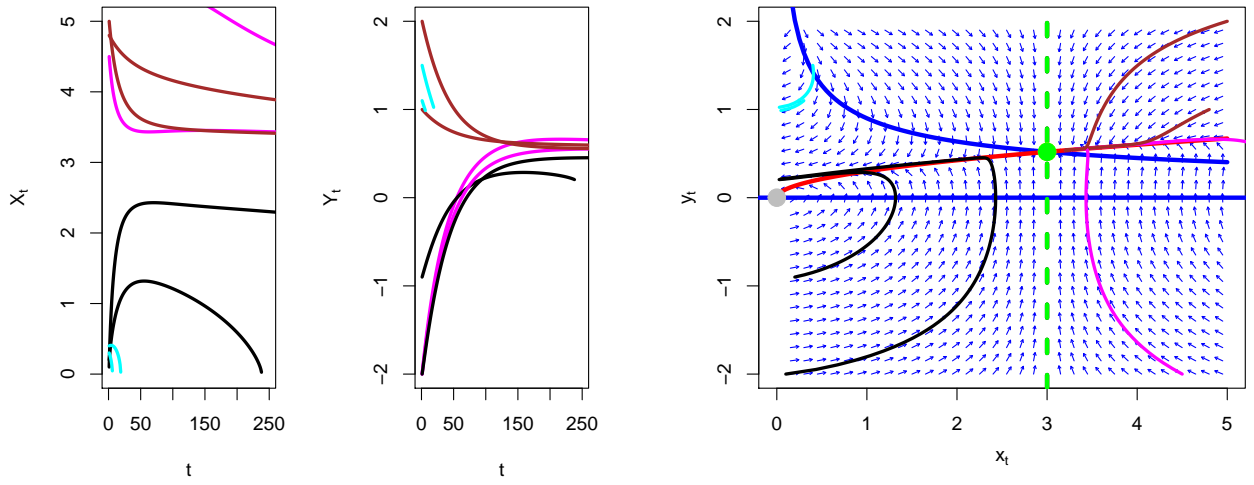


Figure 7: Time series and phase space diagram when $A = K = 3$. The point $(A, u\sqrt{A}) = (K, u\sqrt{K})$ is a saddle.

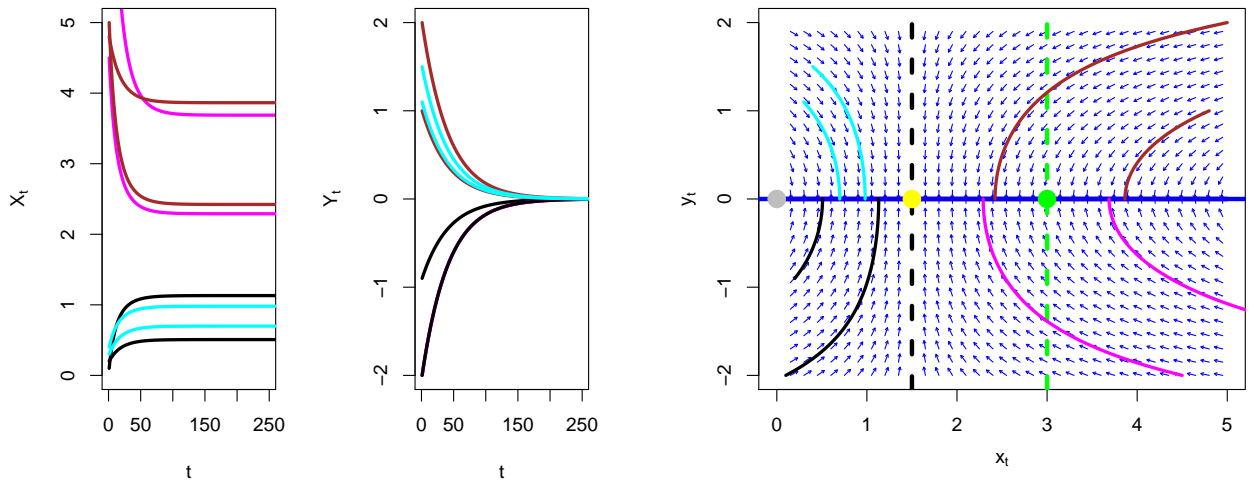


Figure 8: Time series and phase space diagram when $A = 1.5$, $K = 3$, and $u = 0$.

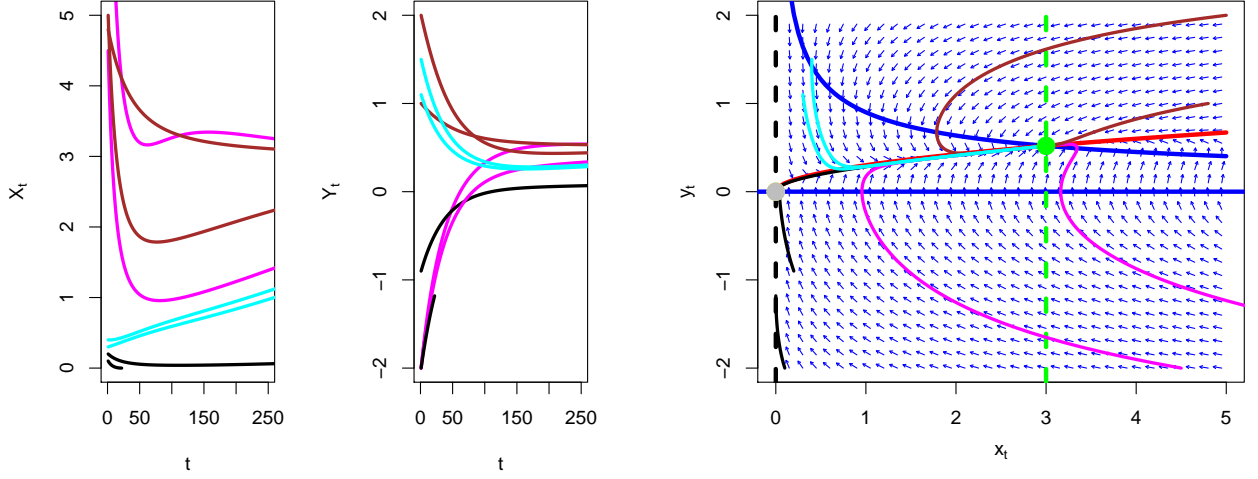


Figure 9: Time series and phase space diagram when $A = 0$ and $K = 3$. The point $(K, u\sqrt{K})$ is an attractor as in the Oja's rule.

3.2 Discussion

In the case of one neuron with non plastic recurrent connection, establishing stability of the steady states is relatively manageable compared to the case of a plastic connection. Figure 5 is similar to a typical case in ecology where the Allee threshold A is less than K . We clearly see that in the region below A , synaptic weights trajectories converge to zero, while postsynaptic neurons trajectories may be either in excitatory or inhibitory states. Interestingly, excitatory postsynaptic neurons never become inhibitory since they never cross the red curve. In that same region, inhibitory neurons become excitatory overtime but with decreasing synaptic weights. Figure 6 shows that if $A > K$, the Allee effect is no more guaranteed to occur below A or even below K . In fact, some neurons, whether in excitatory or inhibitory states would have decaying or increasing synaptic weights. This is the case for the trajectories in black and cyan color. Figure 7 is the case when $A = K$ and there is an Allee effect. Figure 8 is an illustration of the situation where at some point in time, there is no presynaptic activity. Since postsynaptic were already in either excitatory or inhibitory modes, they will decay to zero rather quickly. Figure 9 is essentially the Oja rule and there is no Allee effect.

3.3 Single postsynaptic neuron with one constant recurrent connection

In this case, $\mathbf{Z} = z$ and $\mathbf{v} = v$ are constant with $\frac{d\mathbf{Z}}{dt} = 0$. As we observe above, we consider the system given by

$$\begin{cases} \tau_{\mathbf{w}} \frac{d\|\mathbf{w}\|^2}{dt} &= 2v (\mathbf{W}^T \cdot \mathbf{u} - \frac{v}{K} \|\mathbf{W}\|^2) \left(1 - \frac{A}{\|\mathbf{w}\|^2}\right) \\ \tau_v \frac{dv}{dt} &= -v + T_2(\mathbf{W}, \mathbf{u}, z, v) \end{cases} \quad (3.3)$$

Using the notation $x =: \|\mathbf{W}\|^2$, $y := v$, $u = \|\mathbf{u}\| \cos(\theta)$, and given functions $f_1(x, u)$ and $f_2(x, y, u, v)$, this system is of the form

$$\begin{cases} \tau_x \frac{dx}{dt} &= g_1(x, y) := 2y \left(f_1(x, u) - \frac{yx}{K} \right) \left(1 - \frac{A}{x} \right) \\ \tau_y \frac{dy}{dt} &= g_2(x, y) := -y + f_2(x, y, u, z) \end{cases}. \quad (3.4)$$

This system has similar dynamics to that of the system (3.2). In the linear case where $f_2(x, y, u, z) = u\sqrt{x} + zy$, $\frac{dy}{dt} = (z-1)y + u\sqrt{x} = 0$ if $(1-z)y = u\sqrt{x}$. For $z = 0$, this is the parabola (red solid curve) obtained in the previous case. When z approaches 1, this parabola becomes increasingly “steeped” and eventually explodes into the y -axis when $z = 1$. In the latter case, there is no steady state in the system since they are always given as intersections between the parabola and the vertical lines $x = A$ and $x = (1-z)K$. In reality, there will be infinitely many points of intersection between the parabola and the vertical lines.

3.4 Single postsynaptic neuron with one plastic recurrent connection

For a single postsynaptic neuron with one plastic recurrent connection, we will have $\mathbf{Z} = z$ and $\mathbf{v} = v$. In this paper, we will use Goodall’s rule for its de-correlation properties. For a single neuron, we consider the given by

$$\begin{cases} \tau_{\mathbf{w}} \frac{d\|\mathbf{W}\|^2}{dt} &= 2v \left(\mathbf{W}^T \cdot \mathbf{u} - \frac{v}{K} \|\mathbf{W}\|^2 \right) \left(1 - \frac{A}{\|\mathbf{W}\|^2} \right) \\ \tau_v \frac{dv}{dt} &= -v + T_2(\mathbf{W}, \mathbf{u}, z, v) \\ \tau_z \frac{dz}{dt} &= -(\mathbf{W}^T \cdot \mathbf{u})v + 1 - z \end{cases}. \quad (3.5)$$

Let us now discuss the steady states of the system above:

Case 1: $v = 0$

Then, we would have $T_2(\mathbf{W}, \mathbf{u}, z, v) = 0$, which as above, can only happen if $u = 0$ and $v = 0$. In this case, the third equation suggests that we must have $z = 1$. Thus, in the space formed by $x = \|\mathbf{W}\|^2$, $y = v$, and z , the line parallel to the x -axis with equation $y = 0, z = 1$ is a steady state.

Case 2: $v \neq 0, \mathbf{W}^T \cdot \mathbf{u} = \frac{v}{K} \|\mathbf{W}\|^2$

This condition is equivalent to $v = \frac{K(\mathbf{W}^T \cdot \mathbf{u})}{\|\mathbf{W}\|^2}$.

From the second equation in (3.5), we have $v = \mathbf{W}^T \cdot \mathbf{u} + zv$, therefore, we deduce that $z = 1 - \frac{\|\mathbf{W}\|^2}{K}$.

Using the third equation $-(\mathbf{W}^T \cdot \mathbf{u})v + 1 - z = 0$, it follows that $z = 1 - \frac{\|\mathbf{W}\|^2}{K}v^2$. Since the values of z must be the same value, it follows that we should have $v^2 = 1$. The latter entails having $\|\mathbf{W}\|^2 = K |\mathbf{W}^T \cdot \mathbf{u}|$ and $z = 1 - |\mathbf{W}^T \cdot \mathbf{u}|$. We conclude that there are two steady states in the space formed by $x = \|\mathbf{W}\|^2$, $y = v$, and z , namely, the lines

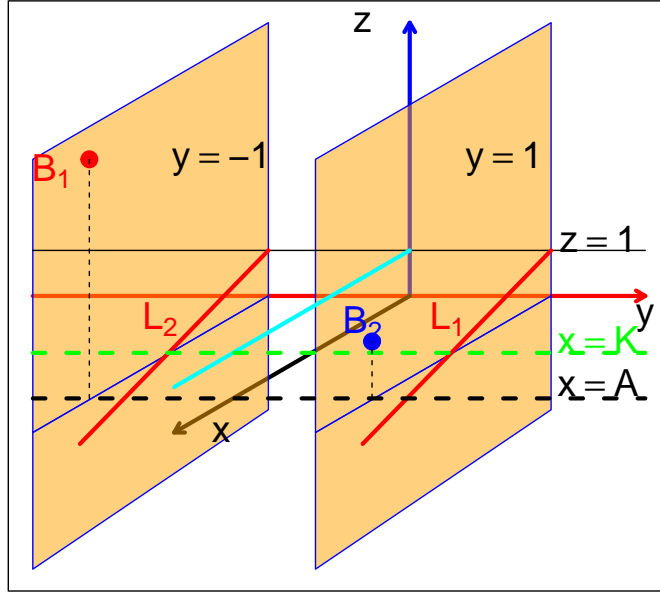
$$L_1 : z = 1 - \frac{x}{K}, \quad y = 1,$$

$$L_2: z = 1 - \frac{x}{K}, \quad y = -1.$$

Case 3: $v \neq 0, \|\mathbf{W}\|^2 = A$

In this case, $v = \mathbf{W}^T \cdot \mathbf{u} + zv$ and thus $v = \frac{\mathbf{W}^T \cdot \mathbf{u}}{1-z}$. We note from above that if $v \neq 0$, then $z \neq 1$. It follows from the third equation of the system (3.5) that, $z = 1 - (\mathbf{W}^T \cdot \mathbf{u})v$, and therefore, we can deduce that $(1-z)(1-v^2) = 0$. Since $z \neq 1$, we must have $v^2 = 1$. The latter implies that $|\mathbf{W}^T \cdot \mathbf{u}| = |1-z|$. Thus $z = 1 \pm \mathbf{W}^T \cdot \mathbf{u}$. We conclude that there are two steady states in the space formed by $x = \|\mathbf{W}\|^2, y = v$, and z , namely, the points

$$B_1 = (A, -1, 1 + u\sqrt{A}), \quad B_2 = (A, 1, 1 - u\sqrt{A}).$$



s

Figure 10: Steady states (in red) of system (3.5), when $A > K$.

Using the notation $x =: \|\mathbf{W}\|^2, y := v, u = \|\mathbf{u}\| \cos(\theta)$, and for given functions $f_1(x, u)$ and $f_2(x, y, z, u)$, the system (3.5) is of the form

$$\begin{cases} \tau_x \frac{dx}{dt} = g_1(x, y, z) := 2y \left(f_1(x, u) - \frac{yx}{K} \right) \left(1 - \frac{A}{x} \right) \\ \tau_y \frac{dy}{dt} = g_2(x, y, z) := -y + f_2(x, y, z, u) \\ \tau_z \frac{dz}{dt} = g_3(x, y, z) := f_3(x, y, u) + 1 - z \end{cases} \quad (3.6)$$

Our first result in this section concerns the stability of the steady state line $x > 0, y = 0, z = 1$ and the points B_1 and B_2 .

Theorem 12. Consider the system (3.6), where $f_1(x, u) = u\sqrt{x}$, $f_2(x, y, z, u) = u\sqrt{x} + zy$, and $f_3(x, y, u) = -uy\sqrt{x}$.

(i) If $u = 0$, then the steady state is the line $(x, 0, 1)$ for $x > 0$ and it is always stable.

(ii) Suppose $u > 0$.

(a) If $u < \frac{2\sqrt{A}}{K}$, then B_1 is unstable and B_2 is stable.

(b) If $u > \frac{2\sqrt{A}}{K}$, then B_1 and B_2 are unstable.

(iii) Suppose $u < 0$.

(a) If $-2\sqrt{A} \max\{2A, K\} \leq u$, then B_1 and B_2 are stable.

(b) If $u < -2\sqrt{A} \max\{2A, K\}$, then B_1 and B_2 are unstable.

(c) If $-2\sqrt{A} \min\{2A, K\} < u < -2\sqrt{A} \max\{2A, K\}$, one of B_1 or B_2 is unstable and the other is stable.

The proof can be found in the Appendix. Our second result discusses the stability of the steady states L_1 and L_2 .

Theorem 13. Consider the system (3.6), where $f_1(x, u) = u\sqrt{x}$, $f_2(x, y, z, u) = u\sqrt{x} + zy$, and $f_3(x, y, u) = -uy\sqrt{x}$. Put

$$\begin{aligned}\alpha_1 &= 2 \left(\frac{u}{2\sqrt{x}} - \frac{1}{K} \right) \left(1 - \frac{1}{A} \right) + 2 \left(u\sqrt{x} - \frac{2x}{K} \right) \left(\frac{A}{x^2} \right), \\ \alpha_2 &= \left(2u\sqrt{x} - \frac{4x}{K} \right) \left(1 - \frac{A}{x} \right), \quad \alpha_3 = 0, \\ \beta_1 &= \frac{u}{2\sqrt{x}}, \quad \beta_2 = -\frac{x}{K}, \quad \beta_3 = -1, \\ \gamma_1 &= \frac{u}{2\sqrt{x}}, \quad \gamma_2 = -u\sqrt{x}, \quad \gamma_3 = -1.\end{aligned}$$

In addition, we let

$$\begin{aligned}a_2 &= (\alpha_1 + \beta_2 - 1), \\ a_1 &= \alpha_1(1 - \beta_2) + \beta_2 - \gamma_2 + \alpha_2\beta_1, \\ a_0 &= \alpha_1(\gamma_2 - \beta_2).\end{aligned}$$

(i) Suppose $a_0 = 0$.

(a) If $a_2^2 + 4a_1 < 0$ and $a_2 < 0$, then L_1 and L_2 are stable.

(b) Suppose $a_2^2 + 4a_1 > 0$.

1. If $a_1 > 0$ and $a_2 > 0$, then L_1 and L_2 are unstable.

2. If $a_1 < 0$ and $a_2 > 0$, then L_1 and L_2 are stable.

3. If $a_1 > 0$ and $a_2 < 0$ or $a_1 < 0$ and $a_2 > 0$, then L_1 and L_2 are unstable.

(ii) If $a_0 < 0$, then L_1 and L_2 are unstable in two cases and stable in one.

(iii) If $a_0 > 0$, then L_1 and L_2 are unstable in case and stable two cases.

The proof can be found in the Appendix

Illustration

Since they are. any cases to consider, we will consider for simplicity just a couple of them for sake of simplicity. In the figures below, we show the dynamics of the system (3.5) above. We choose $M = 20$ different trajectories with length $N = 5000$. The initial state are chosen randomly as: since $x = \|\mathbf{W}\|^2$ must be positive, we randomly select M starting points x_0 in the interval $(0, 5)$. The starting values y_0 are chosen randomly as $M/2 = 10$ in the interval $(-5, 0)$ and $M/2 = 10$ in $(0, 5)$. The starting values z_0 are chosen randomly as $M/2 = 10$ in the interval $(-10, 0)$ and $M/2 = 10$ in $(0, 10)$. The starting points (x_0, y_0, z_0) are the white dots in the figures below. The green sphere is B_1 while the blue sphere is B_2 .

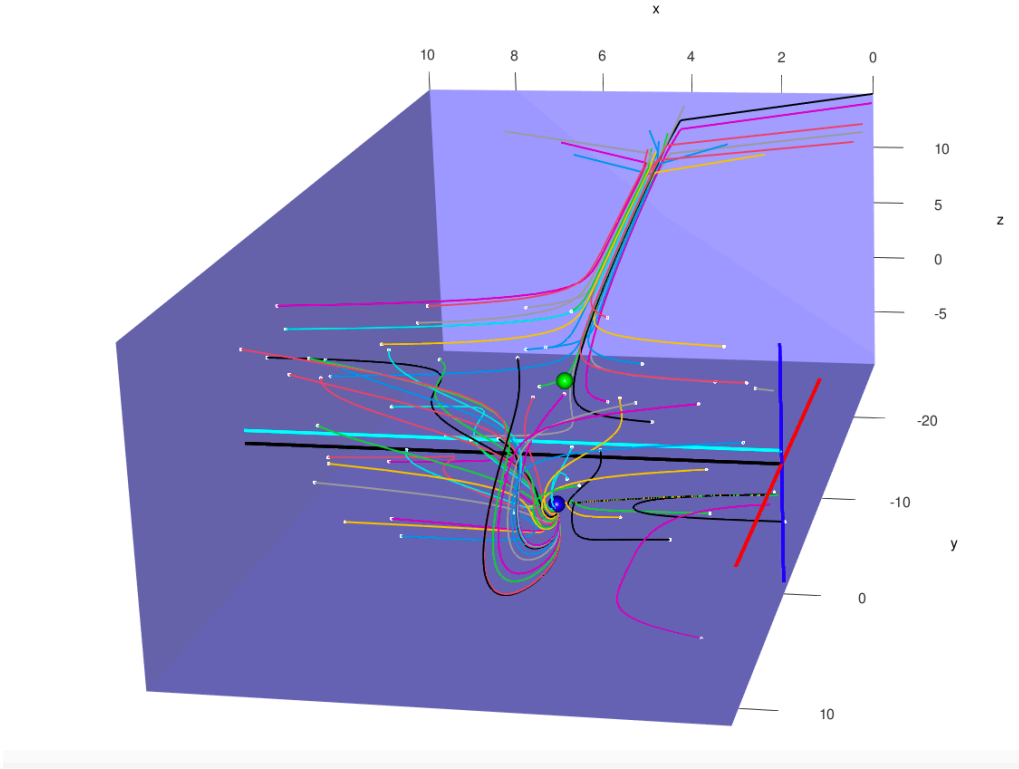


Figure 11: Illustration of the dynamics of the system above for $u = 2, K = 1$, and $A = 4$. $u < \frac{2\sqrt{A}}{K}$ and we observe that B_2 is stable and B_1 is unstable. The cubes $R_1 = [0, 4] \times [0, 10] \times [-5, 0]$ and $R_2 = [0, 4] \times [-20, 0] \times [-5, 10]$ are the Allee regions: starting trajectories will eventually converge to 0 in x leading to absence of plasticity.

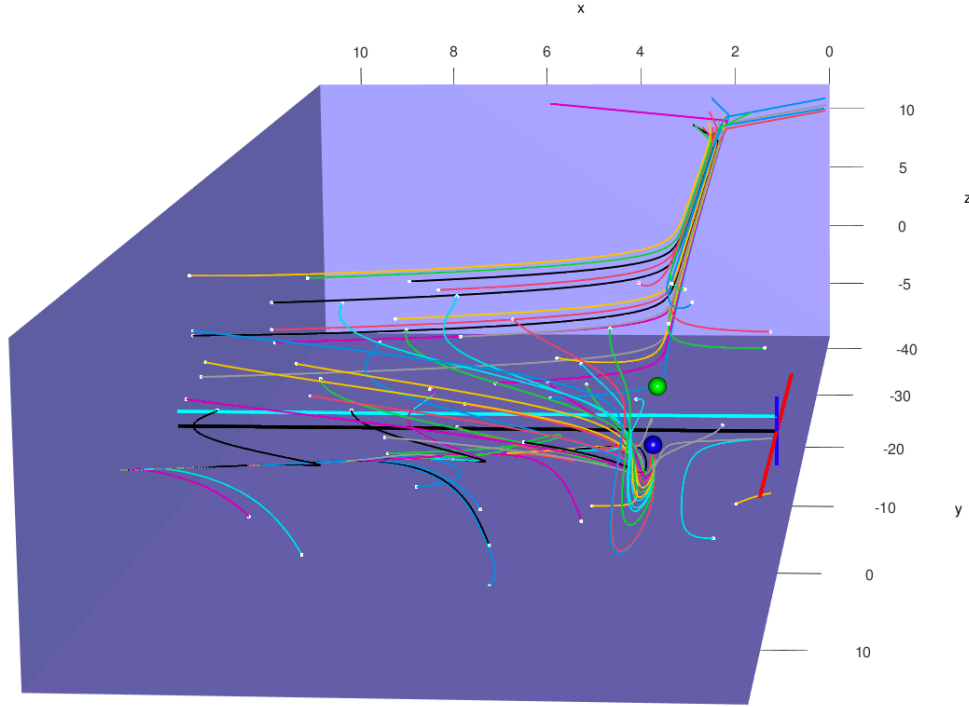


Figure 12: Illustration of the dynamics of the system above for $u = 1.1$, $K = 3$, and $A = 2$. $u > \frac{2\sqrt{A}}{K}$ and we observe that B_1 and B_2 are unstable. In fact, B_1 is clearly a repeller point whereas B_2 is a saddle point. This case is less realistic since synaptic normalization is never achieved. In fact, the lengths of weights x increase without bound while the postsynaptic activities y , though different at early times, become increasing similar overtime (straight line). The Allee regions are the cubes $R_1 = [0, 2] \times [0, 10] \times [-5, 0]$ and $R_2 = [0, 2] \times [-40, 0] \times [-5, 10]$. We observe that the gray trajectory starting just above R_1 does not converge to 0 because it gets into the basin of attraction of L_2 and increases thereafter.

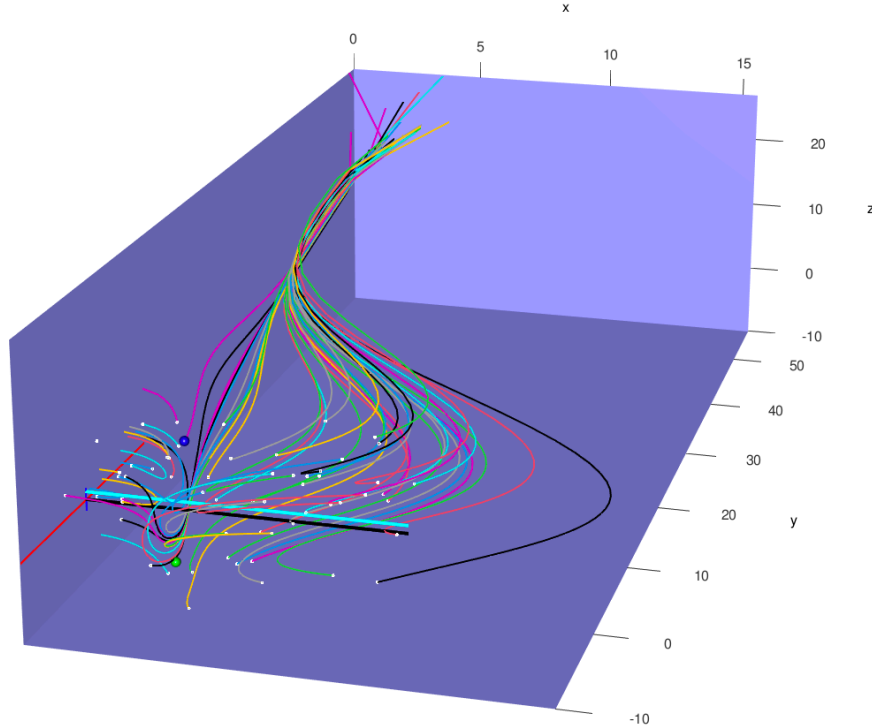


Figure 13: Illustration of the dynamics of the system above for $u = -4$, $K = 4$, and $A = 4$. $u > -2\sqrt{A} \max\{2A, K\}$ and we observe that B_1 and B_2 are unstable. This case is less realistic since synaptic normalization is not achieved all the time. Moreover, postsynaptic activities y and recurrent connections z increase without any bound. If we look close to B_1 and B_2 , we clearly see that no trajectory converges to B_1 and B_2 . The Allee region is cube $R_1 = [0, 4] \times [0, 50] \times [-10, 20]$.

3.5 Discussion

The first simulation shows that lengths of weights x either decrease to $A = 4$ or to 0. The second simulation is more nuanced in that some decrease to $A = 2$ first, then after a while they either decrease to 0 or increase. Others will first increase and then decrease to 0. Finally, some will increase without bound after initially decreasing to close to $A = 2$. What these simulations show is that the size of the Allee regions depend on the value of A . Clearly, if $A = 0$, there is no Allee region and the model is reduced to the Oja rule. An important observation is that since the fixed points B_1 and B_2 both depend on A , the first simulation shows that if $A = 0$ (Oja rule), then weight lengths x all decrease to 0, without any possibility of recovering. This means that, our system while stable in the longterm, represents adrift towards an absence of plasticity. In a sense, the parameter A must positive if we want to have more than a drift towards absence of plasticity for all trajectories.

From above, we clearly see that there is advantage studying the length of weights rather than individual weights. The complexity of the dynamics is vastly reduced. This approach makes studying large amounts of layers mathematically possible while main-

taining interpretability of the results. The main drawback, as illustrated by the results above (Theorem 12 and 13) is that stability analysis, while feasible, still depends unfortunately of complicated quantities.

4 Multiple postsynaptic neurons model

In the single postsynaptic neuron model, we did not include recurrent connections. For a multiple postsynaptic model, we have to consider recurrent connections which themselves maybe fixed or plastic. Another important aspect to consider is that of a layered system where pre-and postsynaptic neurons are on different layers. It is entirely possible that this aspect may help reduce redundancies and correlations among output units.

4.1 Multiple output units with constant recurrent connections

In this case, \mathbf{Z} and \mathbf{v} are nonzero matrices with \mathbf{Z} constant over time. In this case, we fix $1 \leq \ell \leq L$ and $1 \leq j \leq N_v$. The assumption here is still that we have N_u presynaptic neurons and N_v post-synaptic neurons per layer. Now we let $\mathbf{W}_j^{(\ell)}$ be $1 \times N_u$ vector of synaptic weights from the N_u presynaptic neurons $\mathbf{u}^{(\ell)}$ on the ℓ th layer to the j th postsynaptic neurons $v_j^{(\ell)}$ on the ℓ th layer. In this case, equation (3.3)

$$\begin{cases} \tau_{\mathbf{w}_j^{(\ell)}} \frac{d \|\mathbf{W}_j^{(\ell)}\|^2}{dt} &= 2v_j^{(\ell)} \left([\mathbf{W}_j^{(\ell)}]^T \cdot \mathbf{u}^{(\ell)} - \frac{v_j^{(\ell)}}{K_j^{(\ell)}} \|\mathbf{W}_j^{(\ell)}\|^2 \right) \left(1 - \frac{A_j^{(\ell)}}{\|\mathbf{W}_j^{(\ell)}\|^2} \right) \\ \tau_{v_j^{(\ell)}} \frac{dv_j^{(\ell)}}{dt} &= -v_j^{(\ell)} + T \left(\mathbf{W}_j^{(\ell)}, \mathbf{u}^{(\ell)}, z_j^{(\ell)}, v_j^{(\ell)} \right) \end{cases} \quad (4.1)$$

We see that for these given ℓ and j , the system (4.1) has similar dynamics as the system is (3.3). However, there are other considerations to account for in this case. The system's parameters all depend on ℓ and j . The assumptions that time scale constants $\tau_{\mathbf{w}_j^{(\ell)}}$ are the same is not completely unrealistic, especially if the system evolves in a homogeneous ambient space. The same can be said of time scale constants $\tau_{v_j^{(\ell)}}$. The thresholds $A^{(\ell)}$ and $K^{(\ell)}$ can either be the same or can vary, selected according to a chosen distribution. In the constant case, the dynamics of the system (4.1) is identical across all layers, thus the postsynaptic neurons will be perfectly correlated. In the case where these thresholds are not identical, of interest is understanding how and if the thresholds vectors $\mathbf{A}^{(\ell)} = (A_j^{(\ell)})$ and $\mathbf{K}^{(\ell)} = (K_j^{(\ell)})$ for $1 \leq j \leq N_v, 1 \leq \ell \leq L$ affect the correlation between postsynaptic neurons $\mathbf{v}^{(\ell)}$ per layer.

To illustrate the potential effect of thresholds, we will select $N_v = 150$ samples of K from a truncated normal distribution $N(\mu = 0, \sigma^2 = 100)$ over an interval $[1.5, 30]$. Likewise, we will select N_v samples A from an exponential distribution $\exp(\theta = 0.5)$. These distributions are different enough to discriminate potential effect of thresholds A and K . The synaptic weights lengths $x = \|\mathbf{W}\|^2$ will be initialized uniformly over the interval $(0, 5)$. We fix the presynaptic length $u = 0.3$ and we let $z_j^{(\ell)} = 0.4$. The postsynaptic values v will be initialized uniformly within the interval $[-2, 2]$. We will

observe the N_v trajectories of v from $t = 0$ to $t = 25$, because not all of them will converge. In fact, for given N_v postsynaptic neurons, only a $N_v^* \leq N_v$ will converge. We will therefore assess the correlation between these N_v^* trajectories. In Figure 14 (a) below, the heat-map shows that the majority of the $N_v^* = 80$ postsynaptic neurons v are highly correlated. Some of them, albeit a small number are de-correlated. It could be due to the randomness in the choice of the parameters above, or it could be due to the fact that the models itself reduces correlation, without any formal de-correlation mechanism like Goodall's. The boxplots in Figure 14 (b) show the evolution of the N_v^* trajectories overtime. While the distribution of the $N_v^* = 80$ trajectories differ significantly initially, they become increasingly similar over time, despite a few outliers. It also shows that the variance of outputs is constant overtime.

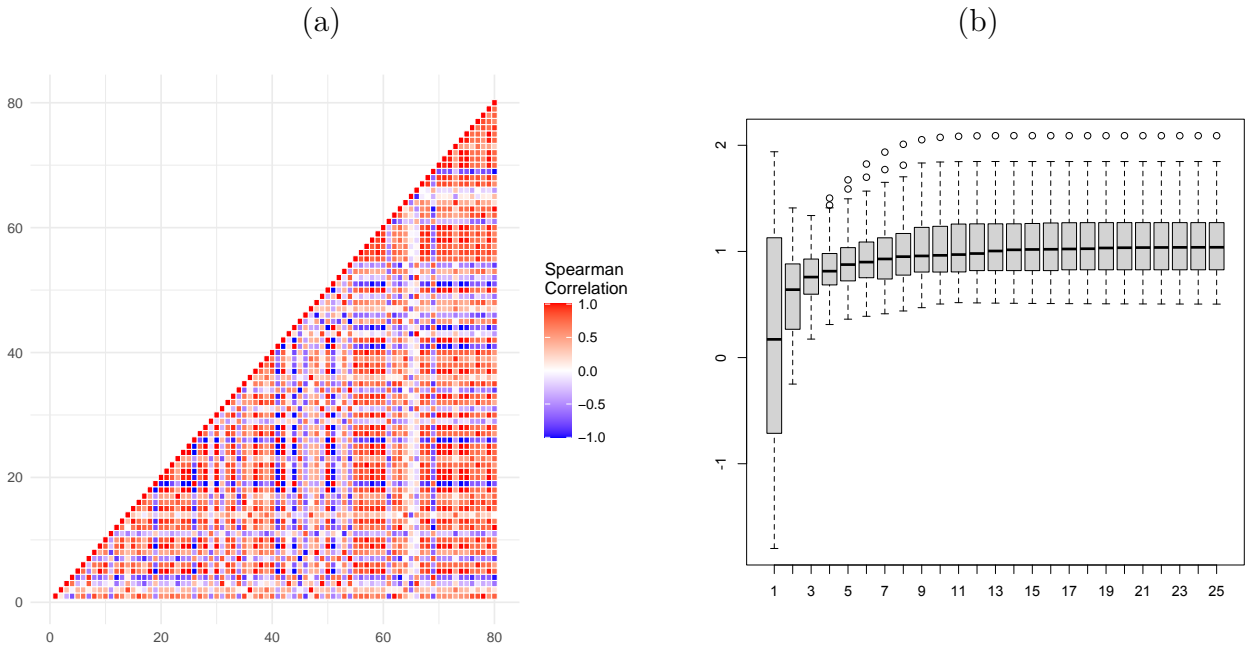


Figure 14: (a) Heatmap showing correlation between the $N_v^* = 80$ convergent trajectories. (b) Boxplots showing the evolution of the distribution of trajectories form time $t = 1$ to $t = 25$.

To ascertain whether the number of de-correlated postsynaptic neuron v is independent of the number N_v chosen, we introduce the de-correlation percentage. There are $\binom{N_v^*}{2}$ Spearman correlation coefficients. The de-correlation percentage is the proportion of these coefficients less than 0.2 (considered a weak correlation in the literature). Figure 15 shows that the de-correlation percentage is high when N_v is low, and decrease with increasing N_v .

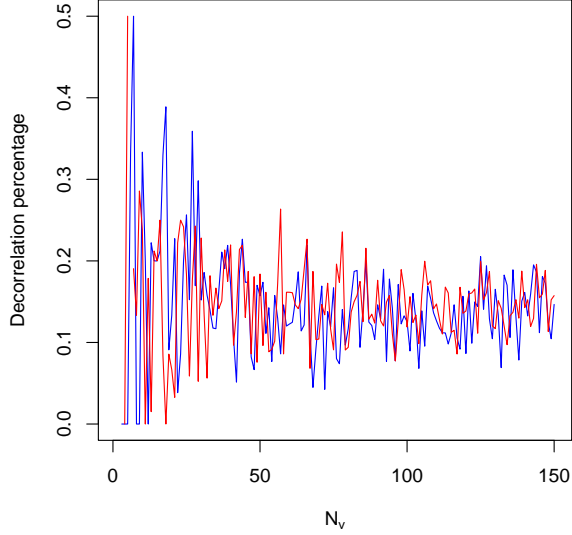


Figure 15: De-correlation percentage for the Oja model (red) and the Allee model (blue), both as functions of the number of postsynaptic neurons per layers N_v .

4.2 Multiple output units with plastic recurrent connections

In this case, \mathbf{Z} and \mathbf{v} are matrices where \mathbf{Z} is time-dependent. As Section 4.1 above, we will fix $1 \leq k, \ell \leq L$ and $1 \leq j, m \leq N_v$. Let $z_{mj}^{(k,\ell)}$ represents the plastic weight connecting the j th postsynaptic neuron $v_j^{(\ell)}$ on the ℓ th layer with the m th postsynaptic neuron $v_m^{(k)}$ on the k th layer. The system (3.5) becomes:

$$\left\{ \begin{array}{l} \tau_{\mathbf{w}_j^{(\ell)}} \frac{d \|\mathbf{W}_j^{(\ell)}\|^2}{dt} = 2v_j^{(\ell)} \left([\mathbf{W}_j^{(\ell)}]^T \cdot \mathbf{u}^{(\ell)} - \frac{v_j^{(\ell)}}{K_j^{(\ell)}} \|\mathbf{W}_j^{(\ell)}\|^2 \right) \left(1 - \frac{A_j^{(\ell)}}{\|\mathbf{W}_j^{(\ell)}\|^2} \right) \\ \tau_{v_j^{(\ell)}} \frac{dv_j^{(\ell)}}{dt} = -v_j^{(\ell)} + T \left(\mathbf{W}_j^{(\ell)}, \mathbf{u}^{(\ell)}, z_{mj}^{(k,\ell)}, v_j^{(\ell)} \right) \\ \tau_{z_{mj}^{(k,\ell)}} \frac{dz_{mj}^{(k,\ell)}}{dt} = - \left([\mathbf{W}_j^{(\ell)}]^T \cdot \mathbf{u}^{(\ell)} \right) v_j^{(\ell)} + 1 - z_{mj}^{(k,\ell)} \end{array} \right. \quad (4.2)$$

As above, we may assume that the ambient space is homogeneous so that time scale constants $\tau_{z_{mj}^{(k,\ell)}}$ are the same. To obtain Figure 16 below, we used the same parameters as in Section 4, with the addition of plastic recurrent connections. The Heatmap in Figure 16 (a), shows that the $N_v^* = 107$ postsynaptic neurons are less correlated than in the previous case above based on the prevalence of light red and light blue colors. Figure 16 (b) shows that the distribution of the trajectories stabilizes relatively quickly compared to the case above.

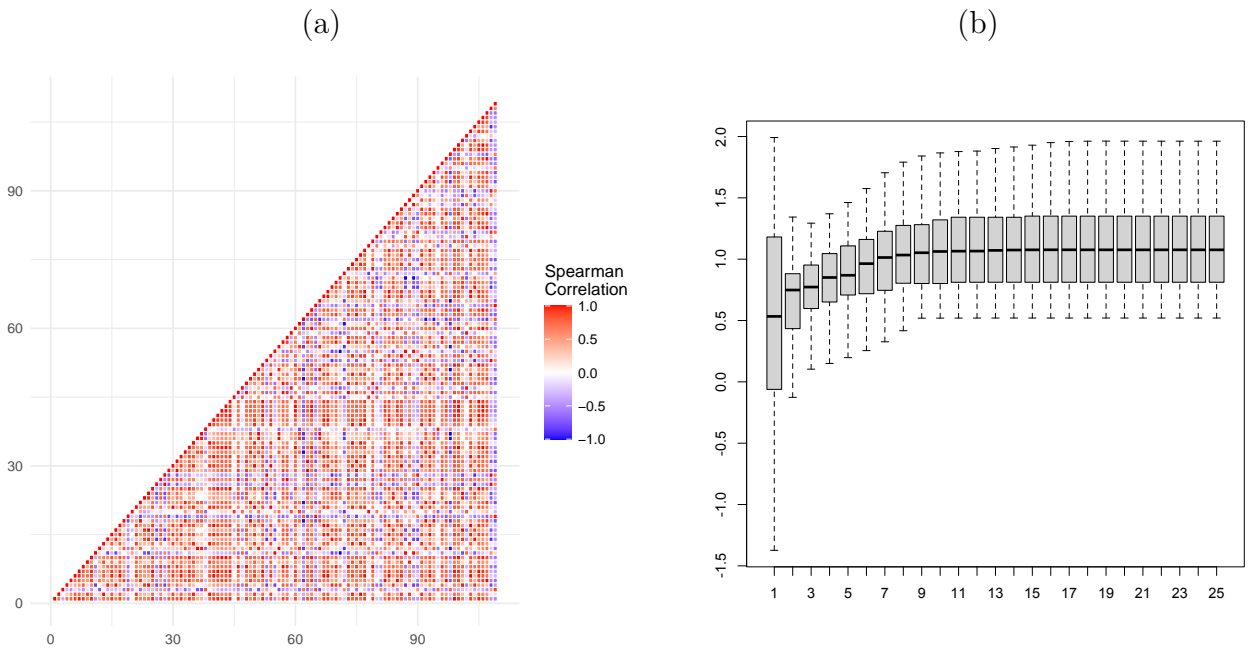


Figure 16: a) Heatmap showing correlation between the $N_v^* = 107$ convergent trajectories. (b) Boxplots showing the evolution of the distribution of trajectories form time $t = 1$ to $t = 25$.

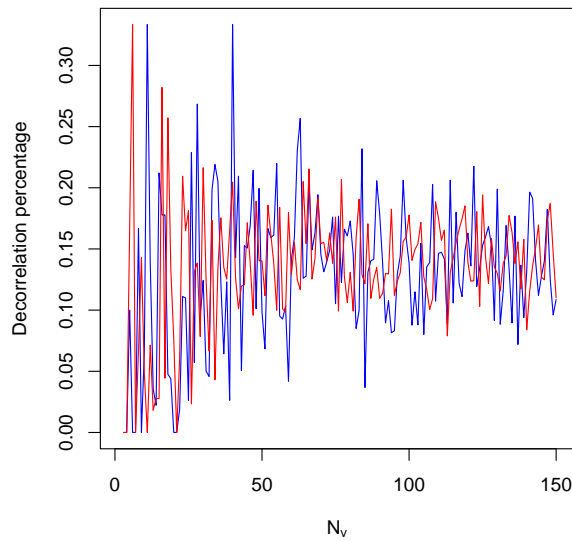


Figure 17: De-correlation percentage for the Oja model (red) and the Allee model (blue), both as functions of the number of postsynaptic neurons per layers N_v .

4.3 Discussion

From the simulations above, we can draw a few observations:

1) The presence of the Allee effect term $(1 - A \|\mathbf{W}\|^{-2})$ in the model overall increases de-correlation, relatively speaking, see Figure 15 above. De-correlation is even increased

when coupled with a de-correlation mechanism such as the Goodall’s method.

2) We selected the thresholds A and K randomly, from noisy distributions so that any measured effects would be independent of their selection. Another important observation is that the initialization of v and \mathbf{Z} does not seem to produce similar results as seen above, even when choosing from heavy-tailed distributions like $N(0, 10)$ or a Student-t with low degrees of freedom.

3) The systems (4.1) and (4.2) are discussed in the context where the time scales are identical per layer. However, if they are chosen to be different and large, then the output units become highly correlated, within layers, reversing the de-correlation gains an Allee term would bring.

4) It seems as though the model, as written in (4.1) and (4.2) may be local to a single chosen layer. However, it is hardly the case given that one can consider that each layer has one single postsynaptic neurons, similarly to discrete dynamics of dynamic neural fields, see Kwessi (2021b).

5 Conclusion

In this paper, we have proposed a definition of the Allee effect in neuroplasticity that maintains the spirit of the Allee effect as originally proposed by Allee (1949). We have also proposed a learning rule that is more general than the Oja learning rule while preserving multiplication normalization, controlling unbounded growth and inducing competition between weights. The model has the advantage that it can accommodate single or multiple pre-and postsynaptic neurons, with and without recurrent connections. Stability analysis was discussed with simulations to illustrate results. Absence of plasticity in the brain can be due to many factors and can be observed in many brain pathologies such as the Alzheimers, stroke, Parkinson’s and Huntington disease. Using the firing-rate equation to model post-synaptic activities could be a limiting factor in the model in that diffusion is not accounted for. A further improvement involving a diffusion term or a lattice differential equation would probably add more nuance and could be worthwhile. In Ecology, remedies to an Allee effect such as immigration have been proposed in Assas et al. (2015a), together with mathematical models explaining the process. This conservationism amounts in practice to adding either new offsprings from different population patches or to controlling predation. In the brain however, it is not clear how one would go about this. Often, neuroscientists focus on reactivating lost or dormant neurotransmitters by using new technologies such as brain implants. While applications of these brain implants have been numerous, mathematical models have lagged or at best, they have been adaptation or reduction of the Hodgkin-Huxley model, see Drapaca (2018). The model we proposed is different and is sensitive to external inputs (as in an Allee-type model) and thus could be used to model the effects of brain implants. From a dynamical systems point of view, the model we propose is complex enough to accommodate a complex structure like the brain. Simulations do show that there are enough parameters in the model to capture a variety of phenomena related to neuroplasticity. From a mathematical point of view, studying the length of weights (rather than individual weights) coupled with other numerical quantities such as postsynaptic signals and their strengths reduces the complexity of the problem while maintaining interpretability of the results. From a purely scientific point of view, the model offers to merge notions

discussed in ecology and neuroscience and it shows that these seemingly isolated areas from each other actually have similarities.

Bibliography

- W. C. Allee. *Principles of Animal Ecology*. W.B. Saunders Co., Philadelphia, 1949. ISBN 0-7216-1120-6.
- L. Assas, S. Elaydi, E. Kwessi, G. Livadiotis, and D. Ribble. Competition models with allee effects. *Journal of Difference Equations and Applications*, 20(8):1127–1151, 2014.
- L. Assas, B. Dennis, S. Elaydi, E. Kwessi, and G. Livadiotis. Hierarchical competition models with the allee effect ii: the case of immigration. *Journal of Biological Dynamics*, 9(1):288–316, 2015a.
- L. Assas, B. Dennis, S. Elaydi, E. Kwessi, and G. Livadiotis. A discrete-time host-parasitoid discrete model with an allee effect. *Journal of Biological Dynamics*, 9(1):34–51, 2015b.
- L. Assas, S. Elaydi, E. Kwessi, G. Livadiotis, and D. Ribble. Hierarchical competition models with allee effects. *Journal of Biological Dynamics*, 9:32–44, 2015c.
- L. Assas, B. Dennis, S. Elaydi, E. Kwessi, and G. Livadiotis. Stochastic modified beverton-holt model with allee effects ii: the cushing-henson conjecture. *Journal of Difference Equations and Applications*, 2016. doi: 10.1080/10236198.2015.107552.
- M. Avery. *A Message from Martha: The Extinction of the Passenger Pigeon and Its Relevance Today*. Bloomsbury, 2014.
- M. F. Bear and R. C. Malenka. Synaptic plasticity: Ltp and ltd. *Curr Opin Neurobiol*, 4:389–399, 1994. ISSN 0959-4388. doi: 10.1016/0959-4388(94)90101-5.
- E. L. Bienenstock, L. N. Cooper, and P. W. Munro. Theory for the development of neuron selectivity: orientation specificity and binocular interaction in visual cortex. *Journal of neuroscience*, 2:32–48, 1982. doi: 10.1523/jneurosci.02-01-00032.1982.
- T.V. Bliss and G. L. Collingridge. A synaptic model of memory: long-term potentiation in the hippocampus. *Nature*, 1997.
- T.V. Bliss and T. Lomo. Long-lasting potentiation of synaptic transmission in the dentate area of the anaesthetized rabbit following stimulation of the perforant path. *J. of Physiol.*, 232:331–356, 1973.
- J. S. Brashares, J. R. Werner, and A. R. E. Sinclair. Social ‘meltdown’ in the demise of an island endemic: Allee effects and the vancouver island marmot. *Journal of Animal Biology*, 79:965–973, 2010. doi: 10.1111/j.1365-2656.2010.01711.x.
- T. Bussey. Pattern separation in the hippocampus: A role for adult neurogenesis and bdnf. *Neuroscience Research*, 71:e35, 2011. doi: 10.1016/j.neures.2011.07.154.

- F. Courchamp, L. Berec, and J. Gascoigne. Allee effects in ecology and conservation. *Oxford University Press, Oxford, Great Britain*, 2008.
- P. Dayan and L. F. Abbott. *Computational and Mathematical Modeling of Neural Systems*. The MIT Press, 2001.
- M. Delitala, , and M. Ferraro. Is the allee effect relevant in cancer evolution and therapy? *AIMS Mathematics*, 5:7648–7659, 2020. doi: 10.3934/math.2020489.
- B. Dennis, L. Assas, S. Elaydi, E. Kwessi, and G. Livadiotis. Allee effects and resilience in stochastic populations. *Theoretical Ecology*, 2015. doi: 10.1007/s12080-015-0288-2.
- J. Dorszewska, W. Kozubski, W. Waleszczyk, M. Zabel, and K. Ong. Neuroplasticity in the pathology of neurodegenerative diseases. *Neural Plast.*, 2020. doi: 10.1155/2020/4245821.
- C. S. Drapaca. Mathematical modeling of a brain-on-a-chip: A study of the neuronal nitric oxide role in cerebral microaneurysms. *Emerging Science Journal*, 2018. doi: 10.28991/esj-2018-01156.
- S. Elaydi, E. Kwessi, and G. Livadiotis. Hierarchical competition models with allee effect iii: Multispecies. *Journal of Biological Dynamics*, 2018. doi: 10.1080/17513758.2018.1439537.
- D. E. Feldman. Developmental synaptic plasticity: Ltp, ltd, and synapse formation and elimination, 2009.
- J. F. Fontanari and L. Perlovsky. Allee effect on language evolution. In *The Evolution of Language - 6th International Conference*, The Evolution of Language - 6th International Conference, 2006.
- E. Fuller. *The Passenger Pigeon*. Princeton University Press, 2014.
- J. Greensberg, editor. *A Feathered River Across the Sky: The Passenger Pigeon's Flight to Extinction*. Bloomsbury, 2014.
- D. O. Hebb. *The Organization of Behavior*. New York: Wiley and Sons, 1949.
- J. A. Hutchings. Thresholds for impaired species recovery. *Proceedings of the Royal Society B*, 282:20150654, 2015. doi: 10.1098/rspb.2015.0654.
- W. James. *The Principles of Psychology. Classics in the History of Psychology*. Green CD, ed, 1890.
- K. E. Johnson, G. Howard, W. Mo, M. K. Strasser, E. A. B. F. Lima, S. Huang, and A. Brock. Cancer cell population growth kinetics at low densities deviate from the exponential growth model and suggest an allee effect. *PLoS Biology*, 17, 2019. doi: 10.1371/journal.pbio.3000399.
- A. Konstorum, T. Hillen, and J. Lowengrub. Feedback regulation in a cancer stem cell model can cause an allee effect. *B. Mathematicakl Biology*, 78:754–785, 2016. doi: 10.1007/s11538-016-0161-5.

- E. Kwessi. A consistent estimator of nontrivial stationary solutions of dynamic neural fields. *Stats*, 4(1):122–137, 2021a.
- E. Kwessi. Discrete dynamics of dynamic neural fields. *Frontiers in Computational Neuroscience*, 2021b. <https://doi.org/10.3389/fncom.2021.699658>.
- P. Z. Liu and R. Nusslock. Exercise and hippocampal neurogenesis: a dogma re-examined and lessons learned. *Neural Reg. Research*, 13:1354, 2018a. doi: 10.4103/1673-5374.235225.
- P. Z. Liu and R. Nusslock. Exercise-mediated neurogenesis in the hippocampus via bdnf. *Front Neurosci.*, 12, 2018b. doi: 10.3389/fnins.2018.00052.
- Z. Neufeld, W. von Witt, D. Lakatos, J. Wang, B. Hegedus, and A. Czirok. The role of allee effect in modelling post resection recurrence of glioblastoma. *Plos Computational biology*, 13:e1005818, 2017. doi: 10.1371/journal.pcbi.1005818.
- E. Oja. Simplified neuron model as a principal component analyzer. *Journal of Mathematical Biology*, 15:267–273, 1982. ISSN 0303-6812. doi: 10.1007/bf00275687.
- A. K. Olson, B. D. Eadie, C. Ernst, and B. R. Christie. Environmental enrichment and voluntary exercise massively increase neurogenesis in the adult hippocampus via dissociable pathways. *Hippocampus*, 16:250–260, 2006. ISSN 1050-9631. doi: 10.1002/hipo.20157.
- T. Perala and A. Kuparinen. Detection of allee effects in marine fishes: analytical biases generated by data availability and model selection. *Proceedings of Royal Society B*, 2017. doi: <https://doi.org/10.1098/rspb.2017.1284>.
- Terrence J. Sejnowski and Gerald Tesauero. The hebb rule for synaptic plasticity: Algorithms and implementations, 1989.
- S.A. Siegelbaum and E. R. Kandel. Learning-related synaptic plasticity: Ltp and ltd. *Curr Opin Neurobiol*, 1:113–120, 1991.
- J. W. Swann and M. Nishimura. Plasticity — dendritic abnormalities in epilepsy, 2009.
- G. W. Thickbroom and F. L. Mastaglia. Plasticity in neurological disorders and challenges for noninvasive brain stimulation (nbs). *J. Neuroeng Rehabil*, 6(4), 2009. doi: 10.1186/1743-0003-6-4.
- F. Viète. Opera mathematica. *F. van Schouten (ed.), Leiden*, 1646.
- G. Voglis and N. Tavernarakis. The role of synaptic ion channels in synaptic plasticity. *Embo Reports*, 2006.
- N. Wang, L. Chen, N. Cheng, J. Zhang, T. Tian, and W. Lu. Active calcium/calmodulin-dependent protein kinase ii (camkii) regulates nmda receptor mediated postischemic long-term potentiation (i-ltp) by promoting the interaction between camkii and nmda receptors in ischemia. *Neural Plast.*, 2014. doi: 10.1155/2014/827161.

V. C. Wimmer, . H. A. Lester, and S. Petrou. Ion channel mutations in familial epilepsy. *Encyclopedia of Basic Epilepsy Research*, pages 651–658, 2009.

J. Xu and J. Kang. The mechanisms and functions of activity-dependent long-term potentiation of intrinsic excitability. *Rev. Neurosci.*, 16:311–323, 2005.

6 Appendix

6.1 Appendix A: Stability analysis of System (3.2)

Proof. Per remark 4 above, we have $y = f_2(x, u) = 0$ for all $x > 0$ only when $u = 0$. Therefore the Jacobian matrix $J(x, 0)$ is given as

$$J(x, 0) = \begin{pmatrix} 0 & 2f_1(x, 0) \left(1 - \frac{A}{x}\right) \\ 0 & -1 \end{pmatrix}.$$

The eigenvalues are therefore $\lambda_1 = 0$ and $\lambda_2 = -1$, which implies that the line $y = 0$ is always a spiral sink.

The partial derivatives of g_1 and g_2 are

$$\begin{aligned} \frac{\partial g_1(x, y)}{\partial x} &= 2y \left(\frac{\partial f_1(x, u)}{\partial x} - \frac{y}{K} \right) \left(1 - \frac{A}{x}\right) + 2y \left(f_1(x, u) - \frac{yx}{K} \right) \left(\frac{A}{x^2} \right), \\ \frac{\partial g_1(x, y)}{\partial y} &= \left(2f_1(x, u) - 4\frac{yx}{K} \right) \left(1 - \frac{A}{x}\right), \\ \frac{\partial g_2(x, y)}{\partial x} &= \frac{\partial f_2(x, u)}{\partial x}, \\ \frac{\partial g_2(x, y)}{\partial y} &= -1 + \frac{\partial f_2(x, u)}{\partial y} = -1. \end{aligned}$$

We are now concerned with the case when $x = A$ and $y = f_2(A, y, u)$. For simplifications purposes, we put $a_0 = f_1(A, u)$ and $b_0 = f_2(A, u)$, $c_0 := \frac{\partial f_2(A, y, u)}{\partial x}$. From above, the Jacobian matrix is given as

$$J(A, b_0) = \begin{pmatrix} 2\frac{b_0}{A} \left(a_0 - b_0\frac{A}{K}\right) & 0 \\ -c_0 & -1 \end{pmatrix}.$$

Since the matrix $J(A, b_0)$ is a lower triangular matrix, the eigenvalues are there $\lambda_1 = 2\frac{b_0}{A} \left(a_0 - b_0\frac{A}{K}\right)$ and $\lambda_2 = -1$. Thus if $b_0(b_0A - a_0K) < 0$, then $\lambda_1 < 0$ and $\lambda_2 < 0$, so the point (A, b_0) is an attractor. If on the other hand $b_0(a_0K - b_0A) \geq 0$, then $\lambda_1 < 0$ and $\lambda_2 > 0$, so the point (A, b_0) is a repeller. Finally, if $(a_0K - b_0A) = 0$, then $\lambda_1 < -1$ and $\lambda_2 = 0$ and then (A, b_0) is a saddle point. \square

Finally, we discuss the case when the steady states are (x, y) with $y = f_2(x, u)$ and $f_1(x, u) = \frac{yx}{K}$. In this case,

$$\begin{aligned} \text{tr}(J) &= \frac{\partial g_1(x, y)}{\partial x} + \frac{\partial g_2(x, y)}{\partial y} \\ &= 2y \left(\frac{\partial f_1}{\partial x} - \frac{y}{K} \right) \left(1 - \frac{A}{x} \right) - 1 + \frac{\partial f_2}{\partial y} \\ &= \frac{2Kf_1}{x} \left(\frac{\partial f_1}{\partial x} - \frac{f_1}{x} \right) \left(1 - \frac{A}{x} \right) - 1 + \frac{\partial f_2}{\partial y}, \end{aligned}$$

and

$$\begin{aligned} \det(J) &= \frac{\partial g_1(x, y)}{\partial x} \frac{\partial g_2(x, y)}{\partial y} - \frac{\partial g_2(x, y)}{\partial x} \frac{\partial g_1(x, y)}{\partial y} \\ &= \frac{2Kf_1}{x} \left(\frac{\partial f_1}{\partial x} - \frac{f_1}{x} \right) \left(1 - \frac{A}{x} \right) \left(-1 + \frac{\partial f_2}{\partial y} \right) + 2f_1 \frac{\partial f_2}{\partial x} \left(1 - \frac{A}{x} \right). \end{aligned}$$

The eigenvalues are

$$\begin{aligned} \lambda_1 &= \frac{1}{2} \left[\text{tr}(J) - \sqrt{\Delta} \right] \\ \lambda_2 &= \frac{1}{2} \left[\text{tr}(J) + \sqrt{\Delta} \right], \end{aligned}$$

where

$$\begin{aligned} \Delta &= [\text{tr}(J)]^2 - 4\det(J) \\ &= \left[\frac{2Kf_1}{x} \left(\frac{\partial f_1}{\partial x} - \frac{f_1}{x} \right) \left(1 - \frac{A}{x} \right) - 1 + \frac{\partial f_2}{\partial y} \right]^2 \\ &\quad - 4 \left[\frac{2Kf_1}{x} \left(\frac{\partial f_1}{\partial x} - \frac{f_1}{x} \right) \left(1 - \frac{A}{x} \right) \left(-1 + \frac{\partial f_2}{\partial y} \right) + 2f_1 \frac{\partial f_2}{\partial x} \left(1 - \frac{A}{x} \right) \right] \\ &= \left[\frac{2Kf_1}{x} \left(\frac{\partial f_1}{\partial x} - \frac{f_1}{x} \right) \left(1 - \frac{A}{x} \right) + 1 - \frac{\partial f_2}{\partial y} \right]^2 - 8f_1 \frac{\partial f_2}{\partial x} \left(1 - \frac{A}{x} \right). \end{aligned}$$

If $\Delta > 0$ with $\det(J) > 0$ and $\text{tr}(J) > 0$, then $\lambda_2 > 0$. In this case, $\sqrt{\Delta} < |\text{tr}(J)| = \text{tr}(J)$ and it follows that $\lambda_1 > 0$. Consequently, we have a repeller (unstable point) at (x, y) such that $y = f_2(x, y, u)$ and $f_1(x, u) = \frac{yx}{K}$.

If $\Delta > 0$ with $\det(J) > 0$ and $\text{tr}(J) < 0$, then $\lambda_1 < 0$. In this case, $\sqrt{\Delta} < |\text{tr}(J)| = -\text{tr}(J)$ and thus $\lambda_2 < 0$. Consequently, we have an attractor (stable point) at (x, y) such that $y = f_2(x, y, u)$ and $f_1(x, u) = \frac{yx}{K}$.

If $\det(J) < 0$, then $\Delta > 0$. If, in addition $\text{tr}(J) > 0$, then $\lambda_2 > 0$. In this case $\sqrt{\Delta} > |\text{tr}(J)| = \text{tr}(J)$ and it follows that $\lambda_1 < 0$. Consequently, we have a saddle at (x, y) such that $y = f_2(x, y, u)$ and $f_1(x, u) = \frac{yx}{K}$.

If $\det(J) < 0$, then $\Delta > 0$. If, in addition $\text{tr}(J) < 0$, then $\lambda_1 < 0$. Since $\sqrt{\Delta} > |\text{tr}(J)| = -\text{tr}(J)$. Therefore $\lambda_2 > 0$. Consequently, we have a saddle at (x, y) such that

$y = f_2(x, y, u)$ and $f_1(x, u) = \frac{yx}{K}$.

We observe in particular that if $x = A$, then $\det(J) = 0$ and one of the eigenvalues λ_1 or λ_2 is 0. The other eigenvalue is positive if $\frac{\partial f_2}{\partial y} > 1$ and negative if $\frac{\partial f_2}{\partial y} < 1$.

6.2 Important particular case

Let us discuss the linear case when $T_1(\mathbf{W}, \mathbf{u}) = \mathbf{u}$ and $T_2(\mathbf{W}, \mathbf{u}, v) = \mathbf{W}^T \cdot \mathbf{u} = \|\mathbf{W}\| \cdot \|\mathbf{u}\| \cos(\theta)$, where θ is the angle between the vectors \mathbf{W} and \mathbf{u} . Therefore $\mathbf{W} \cdot T_1(\mathbf{W}, \mathbf{u}) = \mathbf{W}^T \cdot \mathbf{u}$. This leads to a modified Hebbian rule which becomes the Oja rule if $A = 0$. Using $x := \|\mathbf{W}\|^2$, and $u = \|\mathbf{u}\| \cos(\theta)$, we will have $f_1(x, u) = f_2(x, u) = u\sqrt{x}$. Since x and y have the same dimension, without loss of generality, we can let $\tau_x = \tau_y = 1$.

The steady states for the system (3.3) are $(x, 0)$ for $x > 0$, $(A, u\sqrt{A})$ and $(K, u\sqrt{K})$.

From theorem 10 above, $(x, 0)$, for $x > 0$, is always a spiral sink, which occurs only when $u = 0$.

As for the steady state $(A, u\sqrt{A})$, we have $a_0 = f_1(A, u) = u\sqrt{A}$, $b_0 = f_2(A, y, u) = u\sqrt{A}$, $c_0 = \frac{f_2(A, y, u)}{\partial x} = \frac{u}{2\sqrt{A}}$, and $d_0 = \frac{f_1(A, y, u)}{\partial y} = 0$.

It follows that $1 + d_0 > 0$ and $b_0(a_0K - b_0A) = b_0^2(K - A)$. Therefore, by Theorem ?? above, $(A, u\sqrt{A})$ is a an attractor if $K < A$ and a saddle if $K > A$.

For the steady state $(K, u\sqrt{K})$, we have

$$\begin{aligned} \text{tr}(J) &= \frac{2Kf_1}{x} \left(\frac{\partial f_1}{\partial x} - \frac{f_1}{x} \right) \left(1 - \frac{A}{x} \right) - 1 + \frac{\partial f_2}{\partial y} \\ &= \frac{2Ku\sqrt{x}}{x} \left(\frac{u}{2\sqrt{x}} - \frac{u\sqrt{x}}{x} \right) \left(1 - \frac{A}{x} \right) - 1 \\ &= \left(\frac{Ku^2}{x} - \frac{2Ku^2}{x} \right) \left(1 - \frac{A}{x} \right) - 1 \\ &= - \left[1 + \frac{Ku^2}{x} \left(1 - \frac{A}{x} \right) \right]. \end{aligned}$$

And with $x = K$, we will have:

$$\text{tr}(J) = - \left[1 + u^2 \left(1 - \frac{A}{K} \right) \right].$$

We also have:

$$\begin{aligned} \det(J) &= \frac{2Kf_1}{x} \left(\frac{\partial f_1}{\partial x} - \frac{f_1}{x} \right) \left(1 - \frac{A}{x} \right) \left(-1 + \frac{\partial f_2}{\partial y} \right) + 2f_1 \frac{\partial f_2}{\partial x} \left(1 - \frac{A}{x} \right) \\ &= \frac{2Ku\sqrt{x}}{x} \left(\frac{u}{2\sqrt{x}} - \frac{u\sqrt{x}}{x} \right) \left(1 - \frac{A}{x} \right) (-1) + 2u\sqrt{x} \frac{u}{2\sqrt{x}} \left(1 - \frac{A}{x} \right) \\ &= (-1) \frac{-Ku^2}{x} \left(1 - \frac{A}{x} \right) + u^2 \left(1 - \frac{A}{x} \right) \\ &= u^2 \left(1 - \frac{A}{x} \right) \left(1 + \frac{K}{x} \right). \end{aligned}$$

And with $x = K$, we will have

$$\det(J) = 2u^2 \left(1 - \frac{A}{K}\right).$$

Also,

$$\begin{aligned} \Delta &= \left[\frac{2Kf_1}{x} \left(\frac{\partial f_1}{\partial x} - \frac{f_1}{x} \right) \left(1 - \frac{A}{x}\right) + 1 - \frac{\partial f_2}{\partial y} \right]^2 - 8f_1 \frac{\partial f_2}{\partial x} \left(1 - \frac{A}{x}\right) \\ &= \left[\frac{-Ku^2}{x} \left(1 - \frac{A}{x}\right) + 1 \right]^2 - 8u\sqrt{x} \frac{u}{2\sqrt{x}} \left(1 - \frac{A}{x}\right) \\ &= \left[\frac{-Ku^2}{x} \left(1 - \frac{A}{x}\right) + 1 \right]^2 - 4u^2 \left(1 - \frac{A}{x}\right) \\ &= \left[1 - \frac{Ku^2}{x} \left(1 - \frac{A}{x}\right) \right]^2 - 4u^2 \left(1 - \frac{A}{x}\right) \end{aligned}$$

For $x = K$, we have

$$\Delta = \left[1 - u^2 \left(1 - \frac{A}{K}\right) \right]^2 - 4u^2 \left(1 - \frac{A}{K}\right).$$

Putting $\alpha = u^2 \left(1 - \frac{A}{K}\right)$, then $\Delta = \alpha^2 - 6\alpha + 1$. The roots are

$$\alpha_1 = \frac{6 - \sqrt{32}}{2}, \quad \alpha_2 = \frac{6 + \sqrt{32}}{2}.$$

It follows that $\Delta > 0$ if $\alpha < \alpha_1$ or $\alpha > \alpha_2$ and $\Delta < 0$ if $\alpha_1 < \alpha < \alpha_2$. From Theorem ?? above, we conclude that $x = K$ is either a saddle or an attractor.

6.3 Appendix B: Stability analysis of System (3.6)

6.3.1 Appendix B1

The steady states are obtained when we are on the x -, y -, and z -isoclines. As above, on the x -isocline, we have either $y = 0$, or $f_1(x, u) - \frac{yx}{K} = 0$, or $A = \|\mathbf{W}\|^2$. On the y -isocline, we will have $y = f_2(x, y, z, u)$, and on the z -isocline, we will have $z = 1 - f_3(x, y, u)$. Now we let the Jacobian matrix at a point (x, y, z) be

$$J := J(x, y, z) = \begin{pmatrix} \alpha_1 & \alpha_2 & \alpha_3 \\ \beta_2 & \beta_2 & \beta_3 \\ \gamma_1 & \gamma_2 & \gamma_3 \end{pmatrix}.$$

where

$$\alpha_1 = \frac{\partial g_1(x, y, z)}{\partial x} = 2y \left(\frac{\partial f_1(x, u)}{\partial x} - \frac{y}{K} \right) \left(1 - \frac{A}{x}\right) + 2y \left(f_1(x, u) - \frac{yx}{K} \right) \left(\frac{A}{x^2} \right)$$

$$\begin{aligned}
\alpha_2 &= \frac{\partial g_1(x, y, z)}{\partial y} = \left(2f_1(x, u) - 4\frac{yx}{K}\right) \left(1 - \frac{A}{x}\right), & \alpha_3 &= \frac{\partial g_1(x, y, z)}{\partial z} = 0 \\
\beta_1 &= \frac{\partial g_2(x, y, z)}{\partial x} = \frac{\partial f_2(x, y, z, u)}{\partial x}, & \beta_2 &= \frac{\partial g_2(x, y, z)}{\partial y} = -1 + \frac{\partial f_2(x, y, z, u)}{\partial y} \\
\beta_3 &= \frac{\partial g_2(x, y, z)}{\partial z} = \frac{\partial f_2(x, y, z, u)}{\partial z}, & \gamma_1 &= \frac{\partial g_3(x, y, z)}{\partial x} = \frac{\partial f_3(x, y, u)}{\partial x} \\
\gamma_2 &= \frac{\partial g_3(x, y, z)}{\partial y} = \frac{\partial f_3(x, y, u)}{\partial y}, & \gamma_3 &= \frac{\partial g_3(x, y, z)}{\partial z} = -1.
\end{aligned}$$

In the linear case, we have $f_1(x, u) = u\sqrt{x}$, $f_2(x, y, z, u) = u\sqrt{x} + zy$. With Goodall's model, we will have $f_3(x, y, u) = -uy\sqrt{x}$. It follows that

$$\begin{aligned}
\alpha_1 &= 2y \left(\frac{u}{2\sqrt{x}} - \frac{y}{K}\right) \left(1 - \frac{A}{x}\right) + 2y \left(u\sqrt{x} - \frac{2yx}{K}\right) \left(\frac{A}{x^2}\right) \\
\alpha_2 &= \left(2u\sqrt{x} - 4\frac{yx}{K}\right) \left(1 - \frac{A}{x}\right), & \alpha_3 &= 0 \\
\beta_1 &= \frac{u}{2\sqrt{x}}, & \beta_2 &= z - 1, & \beta_3 &= y \\
\gamma_1 &= \frac{uy}{2\sqrt{x}} = y\beta_1, & \gamma_2 &= -u\sqrt{x}, & \gamma_3 &= -1.
\end{aligned}$$

Now let us discuss the stability of the steady states.

Case 1: Stability of the line $(x, 0, 1)$, $x > 0$.

In this case, we have

$$A_0 := J(x, 0, 1) = \begin{pmatrix} 0 & 2u\sqrt{x} \left(1 - \frac{A}{x}\right) & 0 \\ \frac{u}{2\sqrt{x}} & 0 & 0 \\ 0 & -u\sqrt{x} & -1 \end{pmatrix}.$$

The eigenvalues are

$$\lambda_1 = -1, \quad \lambda_2 = u\sqrt{1 - \frac{A}{x}}, \quad \lambda_3 = -u\sqrt{1 - \frac{A}{x}}.$$

Since $y := v = 0 \implies u = 0$, the eigenvalues are actually

$$\lambda_1 = -1, \quad \lambda_2 = 0, \quad \lambda_3 = 0.$$

Consequently, the line $(x, 0, 1)$ is always stable.

Case 3: Stability of the points B_i , $1 \leq i \leq 2$.

For B_1 , we know that $x = A$, $y = -1$ and $z = 1 + u\sqrt{A}$. In this case,

$$\alpha_1 = -2 \left(\frac{u}{\sqrt{A}} + \frac{2}{K}\right); \quad \alpha_2 = 0, \quad \alpha_3 = 0$$

$$\begin{aligned}\beta_1 &= \frac{u}{2\sqrt{A}}, & \beta_2 &= u\sqrt{A}; & \beta_3 &= -1 \\ \gamma_1 &= -\frac{u}{2\sqrt{A}}; & \gamma_2 &= -u\sqrt{A}, & \gamma_3 &= -1.\end{aligned}$$

Reparametrizing as $\beta = \frac{u}{2\sqrt{A}}$ and $\gamma = u\sqrt{A}$, the Jacobian matrix is given as

$$A_{31} := \begin{pmatrix} \alpha_1 & 0 & 0 \\ \beta & \gamma & -1 \\ -\beta & -\gamma & -1 \end{pmatrix}.$$

$$\lambda_1 = \alpha_1, \quad \lambda_2 = \frac{1}{2} \left[\gamma - 1 + \sqrt{(\gamma - 1)^2 + 8\gamma} \right], \quad \lambda_3 = \frac{1}{2} \left[\gamma - 1 - \sqrt{(\gamma - 1)^2 + 8\gamma} \right].$$

Case 311: $u > 0$.

In this case, $\gamma > 0$, and therefore,

$$\sqrt{(\gamma - 1)^2 + 8\gamma} = \sqrt{\gamma^2 + 6\gamma + 1} = \sqrt{(\gamma + 1)^2 + 4\gamma} \geq |\gamma + 1| = \gamma + 1.$$

It follows that $2\lambda_2 = \gamma - 1 + \sqrt{(\gamma + 1)^2 + 4\gamma} \geq 2\gamma > 0$, and consequently, the point B_1 is unstable.

Case 312: $u < 0$.

In this case, $\gamma < 0$, and therefore, $\lambda_3 < 0$. We also have

$$0 \leq \sqrt{(\gamma - 1)^2 + 8\gamma} \leq |\gamma - 1|.$$

It follows that

$$\gamma - 1 \leq 2\lambda_2 \leq \gamma - 1 + |\gamma - 1|.$$

Since $\gamma < 0 < 1$, we conclude that

$$\gamma - 1 \leq 2\lambda_2 \leq 0.$$

We finally note that $\lambda_1 = \alpha_1 \leq 0$ if $u \geq -\frac{2\sqrt{A}}{K}$. We note that

$$\max \left\{ -\frac{2\sqrt{A}}{K}, -\frac{2\sqrt{A}}{2A} \right\} = -2\sqrt{A} \min \left\{ \frac{1}{2A}, \frac{1}{K} \right\} = -2\sqrt{A} \max \{2A, K\}.$$

We conclude that if $-\frac{2\sqrt{A}}{K} < 2\sqrt{A} \max \{2A, K\} < u < 0$, the point B_1 is stable and if not, it is unstable.

For B_2 , we know that $x = A, y = 1$ and $z = 1 - u\sqrt{A}$. In this case, we have

$$\alpha_1 = 2 \left(\frac{u}{\sqrt{A}} - \frac{2}{K} \right); \quad \alpha_2 = 0, \quad \alpha_3 = 0$$

$$\begin{aligned}\beta_1 &= \frac{u}{2\sqrt{A}}, & \beta_2 &= -u\sqrt{A}; & \beta_3 &= -1 \\ \gamma_1 &= -\frac{u}{2\sqrt{A}}; & \gamma_2 &= -u\sqrt{A}, & \gamma_3 &= -1.\end{aligned}$$

The Jacobian matrix is given as

$$A_{32} := \begin{pmatrix} \alpha_1 & 0 & 0 \\ \beta_1 & -\gamma & -1 \\ \beta_1 & -\gamma & -1 \end{pmatrix}.$$

We find the eigenvalues to be

$$\lambda_1 = 0 \quad \lambda_2 = \alpha_1, \quad \lambda_3 = -\gamma - 1.$$

Case 321: $u > 0$.

In this case, $\lambda_3 < 0$ since $\gamma > 0$. If $u < \frac{2\sqrt{A}}{K}$, then $\lambda_2 = \alpha_1 = 2\left(\frac{u}{\sqrt{A}} - \frac{2}{K}\right) < 0$. It follows that B_2 is stable, if not, it is unstable.

Case 322: $u < 0$.

Then $\lambda_3 = -\gamma - 1 < 0$ if $\gamma > -1$, that is, if $u\sqrt{A} > -1$. Also, $\lambda_2 = \alpha_1 < 0$ if $u < 0$. In conclusion

$$\text{if } -\frac{1}{\sqrt{A}} = -\frac{2\sqrt{A}}{2A} < -2\sqrt{A} \max\{2A, K\} < u < 0, \text{ the point } B_2 \text{ is stable.}$$

6.3.2 Appendix B2

Case 2: Stability of the lines $L_i, 1 \leq i \leq 2$.

For L_1 , we know that $y = 1$ and $z = 1 - \frac{x}{K}$, and

$$\begin{aligned}\alpha_1 &= 2\left(\frac{u}{2\sqrt{x}} - \frac{1}{K}\right)\left(1 - \frac{1}{A}\right) + 2\left(u\sqrt{x} - \frac{2x}{K}\right)\left(\frac{A}{x^2}\right) \\ \alpha_2 &= \left(2u\sqrt{x} - \frac{4x}{K}\right)\left(1 - \frac{A}{x}\right), & \alpha_3 &= 0 \\ \beta_1 &= \frac{u}{2\sqrt{x}} & \beta_2 &= -\frac{x}{K} & \beta_3 &= -1 \\ \gamma_1 &= \frac{u}{2\sqrt{x}}, & \gamma_2 &= -u\sqrt{x}, & \gamma_3 &= -1\end{aligned}$$

The Jacobian matrix is given as

$$A_{21} := \begin{pmatrix} \alpha_1 & \alpha_2 & 0 \\ \beta_1 & \beta_2 & -1 \\ \beta_1 & \gamma_2 & -1 \end{pmatrix}.$$

The characteristic polynomial is $P(-\lambda) = -\lambda^3 + a_2\lambda^2 + a_1\lambda + a_0$. where

$$\begin{aligned} a_2 &= (\alpha_1 + \beta_2 - 1) \\ a_1 &= \alpha_1(1 - \beta_2) + \beta_2 - \gamma_2 + \alpha_2\beta_1 \\ a_0 &= \alpha_1(\gamma_2 - \beta_2) \end{aligned}$$

From Viète's theorem [Viète \(1646\)](#), there are three cases to consider:

Case 21: $a_0 = 0$.

In this case, $P(\lambda) = \lambda(-\lambda^2 + a_2\lambda + a_1)$. The roots are

$$\lambda_1 = 0, \quad \lambda_2 = \frac{1}{2} \left[a_2 - \sqrt{a_2^2 + 4a_1} \right], \quad \lambda_3 = \frac{1}{2} \left[a_2 + \sqrt{a_2^2 + 4a_1} \right].$$

Suppose that $a_2^2 + 4a_1 < 0$. If $a_2 < 0$, then λ_2 and λ_3 are complex conjugates eigenvalues with negative real parts, thus L_1 is stable attractor. If $a_2 > 0$, then L_1 is unstable.

Suppose that $a_2^2 + 4a_1 > 0$. If $a_1 > 0$ and $a_2 > 0$, then λ_2 and λ_3 are real eigenvalues with $\lambda_3 > 0$, thus L_1 is unstable. If $a_1 < 0$ and $a_2 < 0$, then $\lambda_2 < 0$ and $\lambda_3 \leq \frac{1}{2}[a_2 + |a_2|] = 0$. It follows that L_1 is stable. If $a_1 > 0$ and $a_2 < 0$ or $a_1 < 0$ and $a_2 > 0$, then one of the eigenvalues is positive, and thus L_1 is unstable.

Case 22: $a_0 < 0$.

This means that we have 3 cases: 3 negative eigenvalues, 1 negative eigenvalue and 2 complex conjugate eigenvalues, or 2 positive and 1 negative eigenvalues. Clearly, in case the eigenvalues are all negative, L_1 is stable. In the third case, L_1 is unstable. In the second case, L_1 may or may not be stable.

Case 22: $a_0 > 0$.

This means that we also have 3 cases: 3 positive roots, 1 positive eigenvalues and 2 complex conjugate eigenvalues, 2 negative eigenvalues and one positive eigenvalue. In the first and third cases, L_1 is unstable. In the second case, L_1 may or may not be stable.

For L_2 , we know that $y = -1$ and $z = 1 - \frac{x}{K}$. The only difference between this case and the previous is that here,

$$\begin{aligned} \alpha_1 &= -2 \left(\frac{u}{2\sqrt{x}} + \frac{1}{K} \right) \left(1 - \frac{1}{A} \right) + 2 \left(u\sqrt{x} + \frac{2x}{K} \right) \left(\frac{A}{x^2} \right) \\ \alpha_2 &= - \left(2u\sqrt{x} + \frac{4x}{K} \right) \left(1 - \frac{A}{x} \right). \end{aligned}$$